Models of Orientation and Ocular Dominance Columns in the Visual Cortex: A Critical Comparison

E. Erwin*
Beckman Institute, University of Illinois, Urbana, IL 61801 USA

K. Obermayer
The Rockefeller University, New York, NY 10021 USA and
Howard Hughes Medical Institute and Salk Institute, La Jolla, CA 92037 USA

K. Schulten
Beckman Institute, University of Illinois, Urbana, IL 61801 USA

Orientation and ocular dominance maps in the primary visual cortex of mammals are among the most thoroughly investigated of the patterns in the cerebral cortex. A considerable amount of work has been dedicated to unraveling both their detailed structure and the neural mechanisms that underlie their formation and development. Many schemes have been proposed, some of which are in competition. Some models focus on development of receptive fields while others focus on the structure of cortical maps, i.e., the arrangement of receptive field properties across the cortex. Each model used different means to determine its success at reproducing experimental map patterns, often relying principally on visual comparison. Experimental data are becoming available that allow a more careful evaluation of models. In this contribution more than 10 of the most prominent models of cortical map formation and structure are critically evaluated and compared with the most recent experimental findings from macaque striate cortex. Comparisons are based on properties of the predicted or measured cortical map patterns. We introduce several new measures for comparing experimental and model map data that reveal important differences between models. We expect that the use of these measures will improve current models by helping determine parameters to match model maps to experimental data now becoming available from a variety of species. Our study reveals that (1) despite apparent differences, many models are based on similar principles and consequently make similar predictions, (2) several models produce orientation map patterns that are not consistent with the experimental data from macaques, regardless of the plausibility of the models' suggested physiological implementations,

*Present address: Department of Physiology, Box 0444, University of California, San Francisco, San Francisco, CA 94143 USA.

and (3) no models have yet fully accounted for both the local and the global relationships between orientation and ocular dominance map patterns.

1 Introduction

Many cells in the mammalian primary visual cortex are binocular, responding better to stimulation of one eye over the other. They also usually respond more strongly to bars or gratings of one particular orientation (Hubel and Wiesel 1962, 1974). Early experiments with microelectrodes revealed a vertical organization, with columns of cells with similar properties running between pia and white matter, perpendicular to the cortical surface. These experiments also revealed a lateral organization characterized by mostly smooth changes in response properties with lateral distance. The results culminated in the proposal of two seemingly incompatible models of cortical organization—an "icecube" model (Hubel and Wiesel 1977) and a "pinwheel" model (Braitenberg and Braitenberg 1979; Götz 1987).

In recent years, imaging techniques (Blasdel 1992a,b; Blasdel and Salama 1986; Grinvald *et al.* 1986; Ts'o *et al.* 1990) have been developed that allow an increasingly improved characterization of striate cortex organization. A refined picture of map organization has emerged (Bartfeld and Grinvald 1992; Blasdel 1992a,b; Obermayer and Blasdel 1993; Obermayer *et al.* 1992c). We now know that some elements of organization from both the "icecube" and "pinwheel" models are present, but other elements had to be modified in light of the new data. We briefly review the recent findings in the macaque in Section 2.

Along with the study of cortical organization came a series of experiments suggesting that important elements of the organization of orientation and ocular dominance in macaque striate cortex are not prespecified but emerge during an activity-driven, self-organizing process. Occlusion of one eye, for example, leads to dramatic changes in the lateral organization of ocular dominance, which are to some extent reversible. Strabismus leads to changes in the degree of binocularity. Exposure to a restricted set of orientations causes changes in the distribution of cells with different preferred orientations (for reviews see, for example, Hubel *et al.* 1977; LeVay and Nelson 1991; Rauschecker 1991; Stryker *et al.* 1978). These findings as well as an even larger body of data obtained from other species (Goodman and Shatz 1993; Miller 1990) initiated considerable theoretical work in which the principles underlying the development of these patterns were explored. For a recent review see Miller (1990). Many different models have been proposed during the past two decades. However, the different approaches have rarely been thoroughly compared with each other, nor have many of them been tested against the recent experimental data.

Hence it seems timely to critically evaluate the most prominent and successful of the alternative modeling approaches. Such a study serves several purposes: first, it may help to exclude certain approaches; second, it may reveal that seemingly different models are actually related or based on similar principles; third, it may help determine which quantities can be computed to allow model comparisons; and, fourth, it may reveal which of these quantities are most useful for deciding between hypotheses.

In our contribution we make a first step in this direction. We extract principles of organization from recent data obtained from monkey striate cortex and develop numerical tests to demonstrate these properties. We apply these tests to the predictions of a large number of models for the formation of orientation and ocular dominance maps. Model predictions are also compared with available experimental data from the macaque. Several models were found to predict patterns that are inconsistent with the data, and thus are not sufficient models of macaque map structure or development, regardless of the plausibility of the proposed physiological mechanisms. As data become available from more species and under manipulated developmental conditions, the tests developed here will help compare model predictions with such data.

The paper is organized as follows. In Section 2 we briefly review the experimental facts on the patterns of orientation and ocular dominance. In Section 3 we critically evaluate some of the more prominent models, comparing their results with each other and with the experimental data. The discussion is organized around a set of principles we have found to underlie cortical organization. We begin with the two major organizing principles of continuity and diversity that are included in all modeling approaches and continue with less prominent, but equally important features of the map patterns, where differences between models appear. Section 4 summarizes the main results in a table and offers suggestions for future work.

2 Macaque Striate Cortex Orientation and Ocular Dominance Patterns

This section provides a summary of known experimental facts about the lateral organization of orientation and ocular dominance columns in macaque striate cortex. Most of the data being reviewed here were obtained with optical recordings (Blasdel and Salama 1986), since no other method can currently provide both high-resolution data of large surface areas and fairly unambiguous estimates of orientation preferences and ocular dominance in the same animal. Due to limitations of this method, however, data can be obtained only from the superficial layers. When comparing models, one must keep in mind that not all conclusions drawn from these data will necessarily carry over to deeper layers of cortex or be applicable in other species.

This section is included for completeness and cannot treat in depth all the issues involved. For a thorough and quantitative discussion we refer the reader to other sources (Blasdel 1992a,b; Obermayer and Blasdel 1993; Obermayer *et al.* 1992c; Swindale 1992). For experimental data on the cortical mapping of other features such as retinotopy, color sensitivity, and spatial frequency representation obtained by other methods, refer to other sources, e.g., LeVay and Nelson (1991) and Tootell *et al.* (1988), which also include large-scale maps of ocular dominance in all cortical layers (see also Florence and Kaas 1992; Swindale *et al.* 1987).

Figure 1 shows the lateral spatial pattern of orientation selectivity in the striate cortex of an adult macaque. Examples are shown of several elements of the lateral organization that have been termed linear zones, singularities, saddle points, and fractures. Linear zones are characterized by isoorientation contours that run in parallel for distances of 0.5–1.0 mm. Within these zones orientation preferences change linearly with lateral distance along a line. Singularities are point-like regions around which orientation preferences change by 180° along a closed path. Singularities come in two varieties: one where orientation preferences increase with clockwise motion around the center and one where they decrease. Saddle points occur in the centers of regions of almost constant orientation preference. Outward movement within two diagonally opposed quadrants, however, results in the same direction of rotation of orientation preference while outward movement within the remaining quadrants rotates orientation preference in the opposite sense. Finally, fractures are line-like regions across which orientation preferences change rapidly.

Fractures, saddle points, and singularities are grouped together in the recorded patterns (Swindale 1992). They are collectively called nonlinear regions to indicate the reversals and breaks in the pattern of change of orientation preference. Also note that the local direction of the isoorientation contours is independent of the local preferred orientations. This is true in both the linear and nonlinear zones.

Figure 2 shows the lateral spatial pattern of ocular dominance. This pattern was recorded from the same cortical region of the same macaque as in Figure 1. Regions of similar eye dominance are segregated in bands that run in parallel for a considerable distance, but sometimes branch and terminate.

Surprisingly the orientation preference and ocular dominance patterns are not independent as had once been believed (Hubel *et al.* 1978), but are correlated. For example, Figure 3a shows the Fourier transform of the map of orientation preference with an arrow indicating the direction perpendicular to the ocular dominance bands. At least for this region of cortex, the spectrum is characterized by a slightly elliptic band of modes with high amplitude centered around the origin. The minor axis is aligned approximately perpendicular to the ocular dominance band borders. Consequently, the map of orientation is stretched along this axis and it is stretched such that its wavelength along this direction nearly

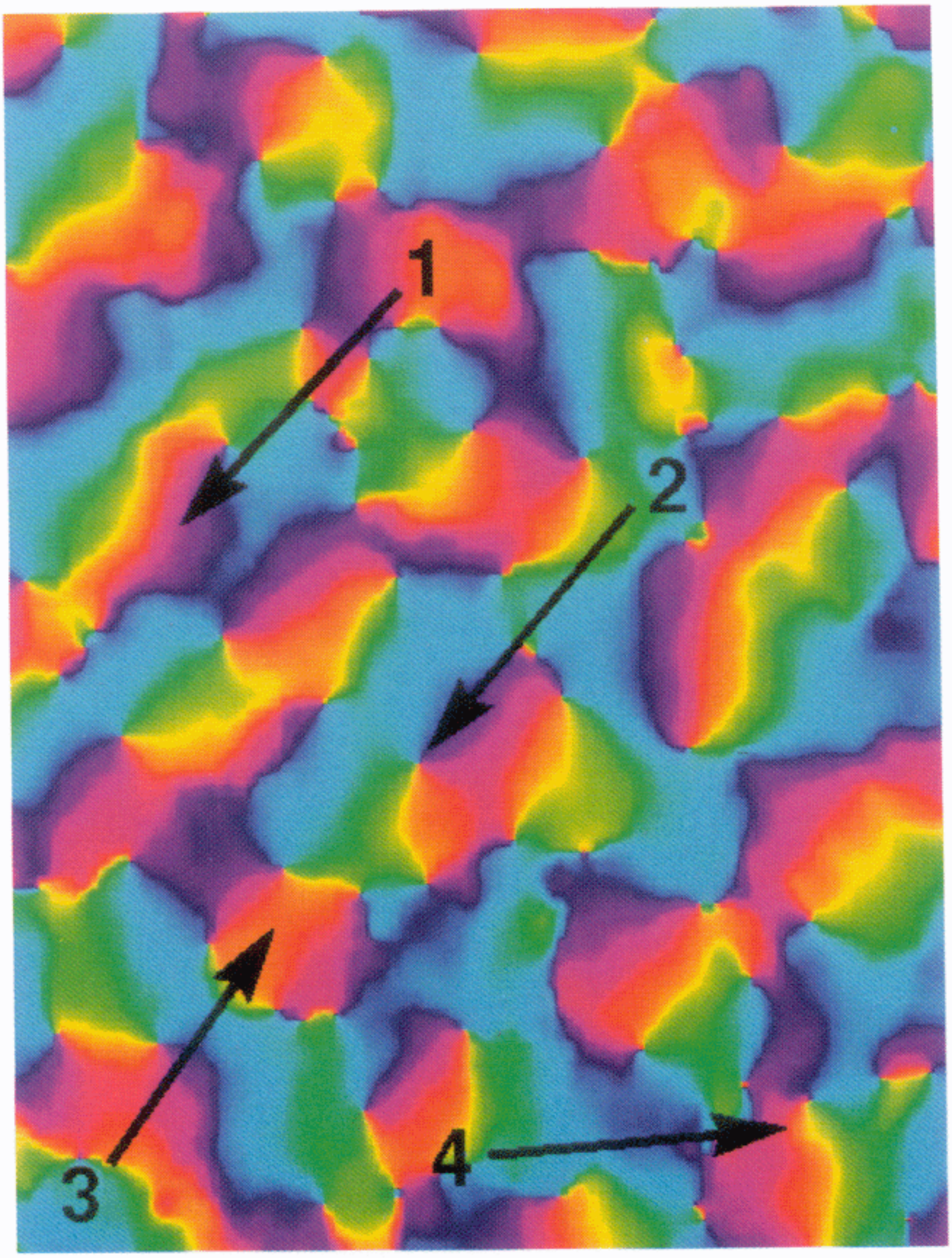

Figure 1: The lateral spatial pattern of orientation preference in the striate cortex of an adult macaque as revealed by optical imaging. The figure (Blasdel 1992a) shows a 4.1 × 3.0 mm surface region located near the border between cortical areas 17 and 18 and close to the midline [animal NM1 in Obermayer (1993)]. Local average orientation preference is indicated by color such that the interval of 180° is mapped onto a color circle. Arrows indicate (1) linear zones, (2) singularities, (3) saddle points, and (4) fractures.

matches the period of the ocular dominance pattern (Obermayer and Blasdel 1993). Additionally, ocular dominance and orientation preference slabs are each aligned with an individual common axis, and these axes—defined as the major axes of the corresponding power spectra—are orthogonal ("global orthogonality") (Obermayer 1993).

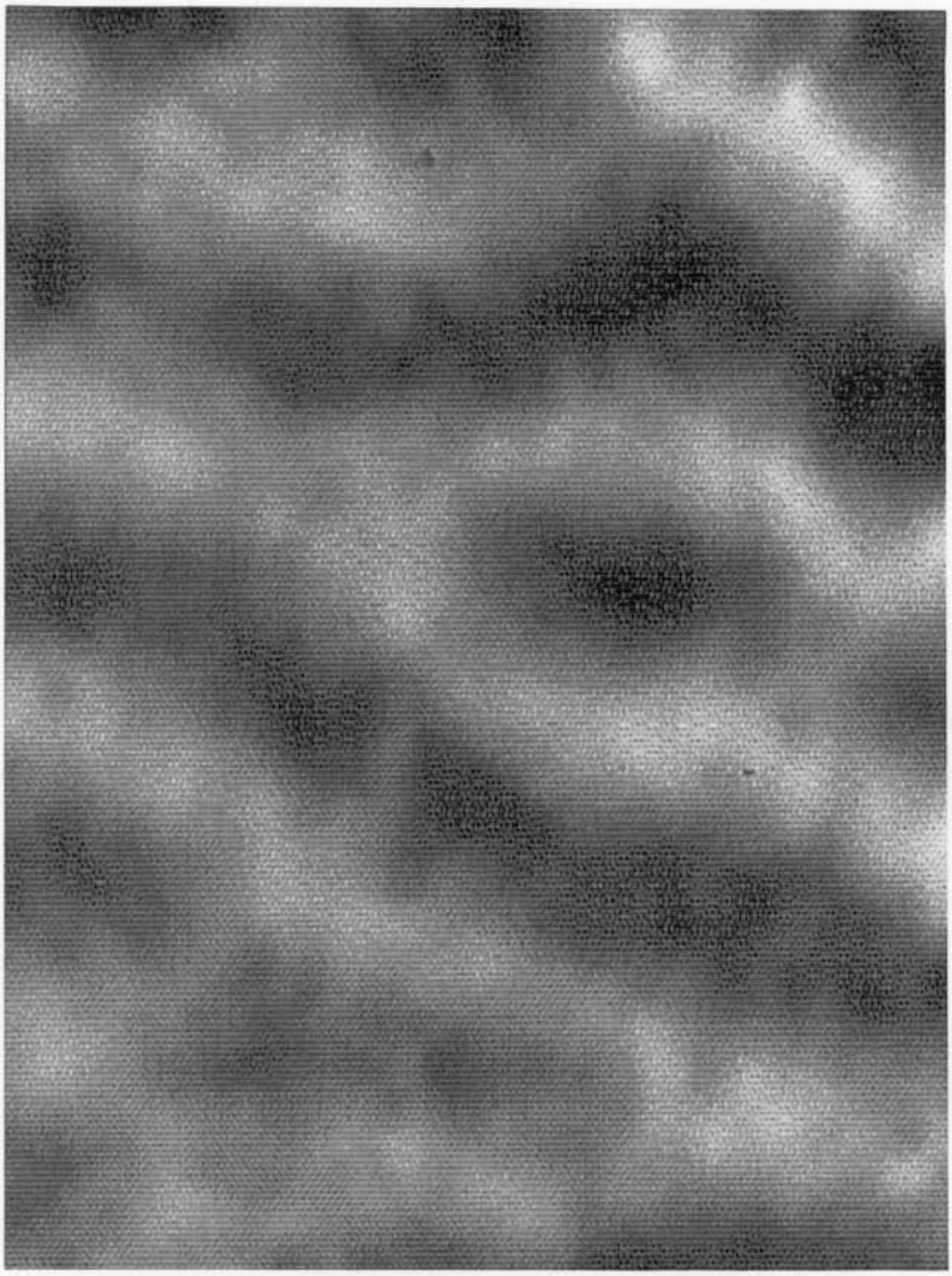

Figure 2: The lateral spatial pattern of ocular dominance in the macaque striate cortex (Blasdel 1992a). Dark and light regions are dominated by input from contralateral and ipsilateral eyes, respectively. Data were obtained from the same cortical region of the same animal (NM1) as in Figure 1.

Other correlations become apparent in a contour plot representation. Figure 4 displays a contour plot of the orientation map from Figure 1 overlaid with the borders of the ocular dominance bands from Figure 2. Three properties of this pattern are noteworthy: (1) singularities tend to align with the centers of ocular dominance bands; (2) saddle-points align, too; and (3) isoorientation contours intersect borders of ocular dominance bands at angles of approximately 90° locally, on a scale as fine as the small meanderings of the ocular dominance bands ("local orthogonality"). For a quantitative analysis, see Blasdel *et al.* (1994) and Obermayer and Blas-

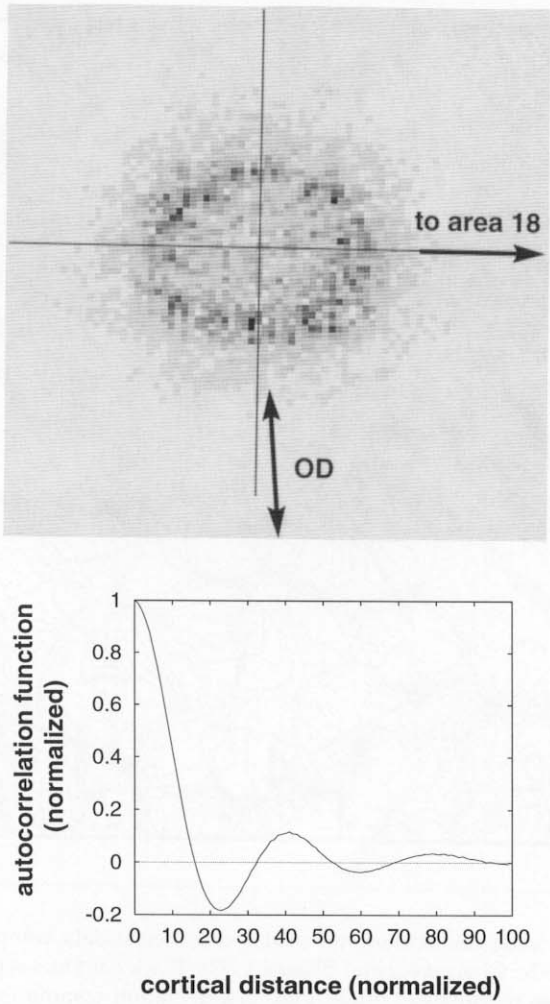

Figure 3: (a) The complex Fourier power spectrum of the spatial pattern of orientation preference $\|f(\mathbf{k})\|^2$, $f(\mathbf{k}) = \sum_{\mathbf{r}} \exp(i\mathbf{kr}) q(\mathbf{r}) \{\sin[2\phi(\mathbf{r})] + i \cos[2\phi(\mathbf{r})]\}$ recorded from another macaque [NM4 in Obermayer (1993)]. The arrows indicate the direction perpendicular on average to the borders of the ocular dominance bands, and the direction perpendicular to the border to area 18. (b) Normalized autocorrelation function of preferred orientation as a function of distance. The figure shows the autocorrelation function for one of the Cartesian components of the orientation vector. One hundred units of cortical distance correspond to 1.252 mm.

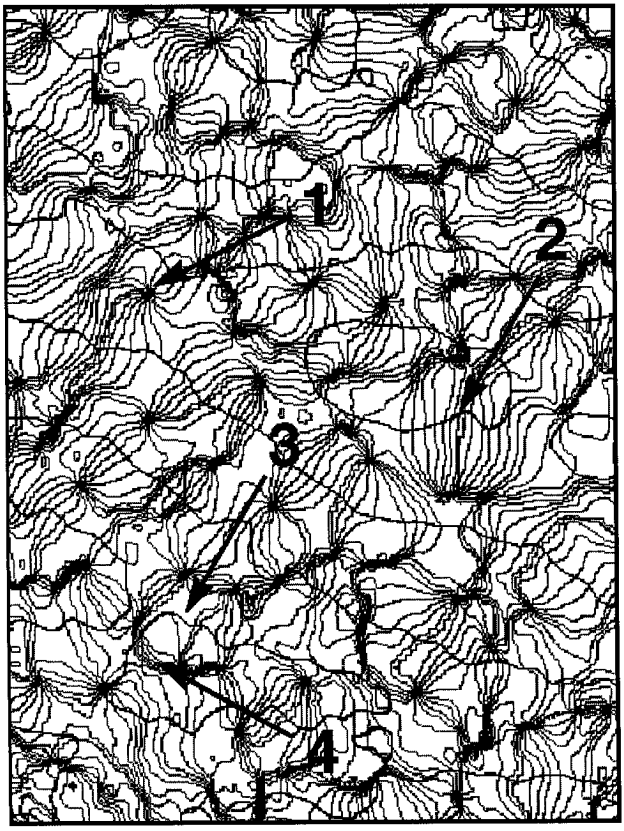

Figure 4: Macaque orientation and ocular dominance data combined (Obermayer *et al.* 1992c; Obermayer and Blasdel 1993). Black contours separate bands of opposite eye dominance. Light gray isoorientation contour lines indicate intervals of 11.25°. The medium gray contour represents the preferred orientation 0°. Arrows indicate (1) singularities, (2) linear zones, (3) saddle points, and (4) fractures.

del (1993). Correlations have also been reported for fractures, which tend either to align with the centers of ocular dominance bands or to run perpendicular to their borders (Blasdel and Salama 1986). Also, regions in the centers of ocular dominance bands tend to be less specifically tuned to their preferred orientation than regions that receive balanced input from both eyes (Blasdel 1992b; Livingstone and Hubel 1984).

Despite the correlations between them, both ocular dominance and orientation preference patterns exhibit irregularities and "global disorder." Such disorder is exhibited in the locally varying width of the ocular dominance bands as well as in their irregular termination and branching pattern. Figure 3b illustrates the presence of disorder in the orientation maps with an autocorrelation function along the Cartesian coordinates of orientation preference. The autocorrelation function takes a Mexican-hat shape with orientation preferences anticorrelated for distances around 300 μm. For neurons separated by longer distances, correlations decay to zero after a few oscillations indicating global disorder.

3 Common Properties of Cortical Map Models

Many models for the structure and formation of orientation and ocular dominance maps have been proposed. Although seemingly based on different assumptions, most produce maps that visually resemble the experimentally obtained maps. To sort through the conflicting models we extended and analyzed some of the more prominent of the previously proposed models and compared their predictions with the experimental data.

We found that models that appear to be based on different principles share many assumptions, and that these assumptions have a great impact on the developed patterns. The following discussion is organized around a list of these common assumptions, moving from the most generic to the most specific. Increasingly detailed comparisons between model and experimental data will be included along with each point.

To ease comparisons, we group models into categories based on similarities in goals or implementation (Table 1). Structural and spectral models attempt to characterize map patterns using schematic drawings or concise equations. In structural models this description is formulated in real space, while spectral models are formulated in Fourier space.

As model complexity increases, the pattern-generating equations are meant to correspond more closely to actual physiological processes, revealing more clearly the mechanisms underlying pattern formation. Correlation-based learning models involve Hebbian learning and linear intracortical interactions, while competitive Hebbian models are based on nonlinear lateral interactions. Several models do not fit well in these categories. The "generalized deformable" model of Yuille *et al.* (1991), for example, includes aspects of both competitive Hebbian and correlation-based learning models. Brief mathematical descriptions of some of the models discussed are included in the Appendix.

3.1 Basic Assumptions. Models of cortical map formation and structure include a collection of neural units in a model cortical array, usually on a two-dimensional grid. Usually each model neuron represents not

Table 1: Categories of Models of Visual Cortical Maps, and Their Abbreviations as Used in This Article.[a]

Class	Model	Reference
Structural models	Icecube	Hubel and Wiesel (1974)
	Pinwheel	Braitenberg and Braitenberg (1979)
	Götz	Götz (1987)
	Baxter and Dow	Baxter and Dow (1989)
Spectral models	Rojer and Schwartz	Rojer and Schwartz (1990)
	Niebur and Wörgötter	Niebur and Wörgötter (1993)
	Swindale	Swindale (1992a)
Correlation-based learning	Linsker	Linsker (1986c)
	Miller	Miller *et al.* (1989), Miller (1992, 1994)
Competitive Hebbian	SOM-h	Obermayer *et al.* (1990)
	SOM-l	Obermayer *et al.* (1992c)
	EN	Durbin and Mitchison (1990)
Other	Tanaka	Tanaka 1991b, Miyashita and Tanaka (1992)
	Yuille *et al.*	Yuille *et al.* (1991)

[a]Two versions of the self-organizing map model were investigated: SOM-h (high-dimensional weight vectors) and SOM-l (low-dimensional feature vectors).

one real neuron, but a collection of real neurons located in a cortical column or in a single layer of cortex. Each model neuron has a receptive field associated with it that defines how it responds to different types of simulated visual input.

Properties of receptive fields are often described through preferences for certain stimulus features, which in turn can be represented in various ways. The two most common ways to represent feature preferences are feature vectors and synaptic weight vectors.

In the feature vector representation, feature preferences are represented by a low-dimensional vector with independent components representing such features as ocular dominance, orientation preference, retinotopic position, or preferred direction in color space. In the weight vector representation a weight vector codes for the effective strength of the connections between a (simple) cortical cell and a set of receptor cells in an input layer. In these models, the weight vectors act as linear filters on the distribution of input activity. Receptive fields are defined by the strengths of the connections, and the locations and properties of the input cells.

It has been suggested that receptive fields be described not only as spatial filters but as spatiotemporal filters (e.g., Adelson and Bergen 1985; Emerson *et al.* 1992). Other suggestions aim at the inclusion of nonlinearities (Lehky *et al.* 1992) to account for complex cells, cells in higher brain areas, or intracortical feedback (Reggia *et al.* 1992; Sirosh and Miikku-

lainen 1994). These more realistic representations, however, have not yet been extensively used in models of cortical map structure and formation.

The method chosen to represent feature preferences will necessarily introduce assumptions about which features of visual input are important and hence influence model predictions. Abstract feature vectors allow one to generalize models to describe several phenomena within the same framework, but require that the types of features to be represented be fully determined in advance. Receptive fields represented with high-dimensional weight vectors can often be scrutinized for additional feature preferences beyond those for which the model was designed. High-dimensional models may also be explained with less abstracted physiological principles. However, they require greater computational resources and thus must generally be limited in other ways, such as through linear development rules, lower cortical resolution, and fewer simultaneous feature preferences.

3.2 Continuity and Diversity. It has long been recognized that two fundamental characteristics of orientation and ocular dominance organization are continuity and diversity (e.g., Baxter and Dow 1989; Obermayer *et al.* 1990; Swindale 1982).

Continuity stresses the fact that nearby columns of cells in striate cortex tend to prefer stimuli with similar features. Similarity between feature preferences is commonly defined as a small distance between their associated feature vectors calculated via a suitable norm. Models often enforce continuity by combining feature preferences of nearby cells through averaging or convolution operations, usually invoking a linear similarity measure by linearly averaging over each vector component individually. Other similarity measures are possible. The choice of similarity measure will affect the resulting map patterns (Yuille *et al.* 1991).

Diversity states that the space of all possible feature preferences should be filled as completely as possible, thus avoiding "perceptual scotomata" (Swindale 1991). Diversity is often enforced by bandpass filtering of the spatial pattern of feature preferences (Niebur and Wörgötter 1993; Rojer and Schwartz 1990), sometimes implemented using competitive networks (Durbin and Mitchison 1990; Obermayer *et al.* 1990, 1992c).

The two principles of continuity and diversity are partially contradictory and are balanced in visual maps. There are some regions where continuity is violated, such as the singularities and sharp fractures in the orientation preference map. Similarly there are regions where continuity is stressed over diversity. For example, the full range of orientation preferences is not represented near the saddle points.

The continuity and diversity principles have been the fundamental principles of almost all descriptive and developmental models of orientation or ocular dominance map patterns. They were already implemented in both Hubel and Wiesel's original icecube model (Hubel and Wiesel 1977) and in the early pinwheel models (Braitenberg and Brait-

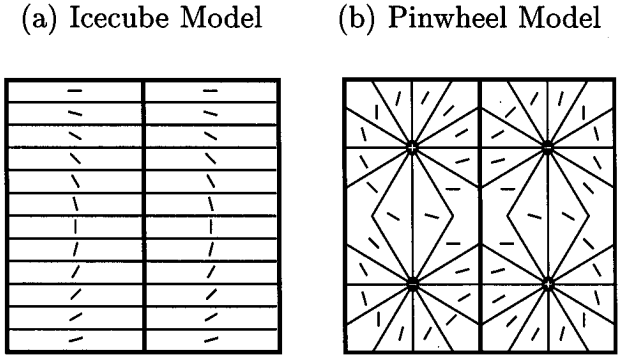

Figure 5: Schematic illustrations of two competing structural models. Heavy borders and shading define columns of cells with opposite eye preference; light borders separate columns of cells with similar preferred orientations, indicated by short lines. (a) The icecube model of cortical organization (Hubel and Wiesel 1974). (b) Götz' (1987) modified version of Braitenberg and Braitenberg's pinwheel model (1979). Positive and negative singularities are indicated by "+" and "−" where orientation preferences increase (decrease) with counterclockwise movement around the center of positive (negative) vortices.

enberg 1979; Götz 1987) (Fig. 5). However, maps from certain models that follow both of these principles may still differ in qualitative ways from experimental data. For example, the icecube model obeys the principles of continuity and diversity, but contains no singularities in the orientation preference map and no branching or termination of ocular dominance bands. Thus additional principles must be introduced. Some of these principles will be seen as modifications of the ideas of continuity and diversity.

3.3 Global Disorder. There are certain characteristic local features of cortical maps that recur in all regions of the maps. However, cortical maps do not consist of a crystal-like grid of exactly repeating units. Rather the maps are characterized by the liquid-like properties of local correlations and the absence of long-range order. These properties are reflected in the autocorrelation functions (Fig. 3b) of orientation and ocular dominance with respect to distance along the map surface.[1] Note that the principle of global disorder is distinct from the principle of diversity. Models with feature preferences arranged in a repeating patchwork

[1]The global disorder observed in cortical maps is the outcome of developmental processes and is not simply due to a folding of the cortical surface.

(Bauer and Dow 1991; Braitenberg 1985; Braitenberg and Braitenberg 1979; Dow and Bauer 1984; Götz 1987) meet both the continuity and diversity constraints, but do not show global disorder.[2]

Global disorder can be implemented in several ways. In some of the structural models it arises due to the explicit inclusion of noise (Niebur and Wörgötter 1993; Rojer and Schwartz 1990; Swindale 1982, 1992). The underlying assumption is that the map-organizing process is analogous to bandpass filtered white noise and the maps are consequently fully characterized by the filter parameters. Filtering is implemented either in the spatial domain by convolving arrays of randomly oriented vectors (Swindale 1982, 1992) with Mexican-hat type kernels or in the Fourier domain by multiplying white noise with a bandpass filter (Niebur and Wörgötter 1993; Rojer and Schwartz 1990). Continuity and diversity arise by suppressing both high- and low-frequency Fourier modes; global disorder results from applying the filter to white noise. The success of these models (Fig. 6) effectively suggests that the underlying principles of continuity, diversity, and global disorder are the most important principles of map structure.

Other models lead to a stationary state by an iterative process (Durbin and Mitchison 1990; Goodhill and Willshaw 1990; Miller 1992; Miller *et al.* 1989; Obermayer *et al.* 1992c; Swindale 1982, 1992). Usually there are many possible stationary states. The overwhelming majority of these tend to lack global order because of degeneracies due to translational symmetry[3] in the underlying pattern-generating equations or due to frustration (Swindale 1982, 1992). Random choice of initial conditions and/or randomly directed movement in the state space, e.g. in response to random inputs (Durbin and Mitchison 1990; Obermayer *et al.* 1990, 1992c), effectively cause a random choice of one of these stationary states. It is overwhelmingly probable that this stationary state will lack long-range order.

In competitive Hebbian models (Durbin and Mitchison 1990; Obermayer *et al.* 1990, 1992c), for example, an isotropic power spectrum and Fourier eigenmodes are generated since the pattern-generating equations are invariant under both translations and rotations. Similarity is enforced by modifying the feature vectors of cells only in groups of neighboring cells, moving them all closer to a presented input pattern. Diversity is the result of competition, implemented as a selection rule in the self-organizing map (Obermayer *et al.* 1990, 1992c), and by a softmax nonlinearity in the elastic net (Durbin and Mitchison 1990). Presenting the

[2]Models that introduce periodic boundary conditions as a convenience are not intended to imply that cortical patterns are periodic, and thus do not necessarily violate the principle of global disorder.

[3]If the equations governing development are invariant under translation in cortical and retinal coordinates, then Fourier transform leads to a set of independent equations, one for each Fourier mode. If each of those equations has more than one stationary state, the number of stationary states for the whole system is huge.

(a) Swindale's Model, $a \neq 0$

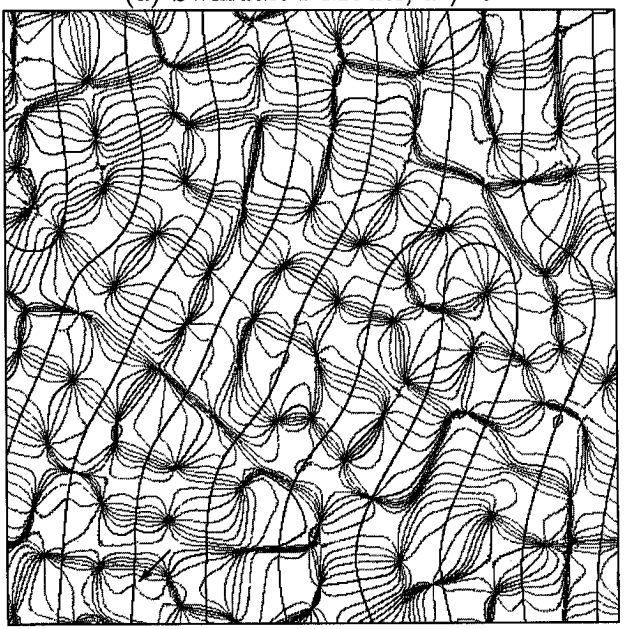

(b) Swindale's Model, $a = 0$

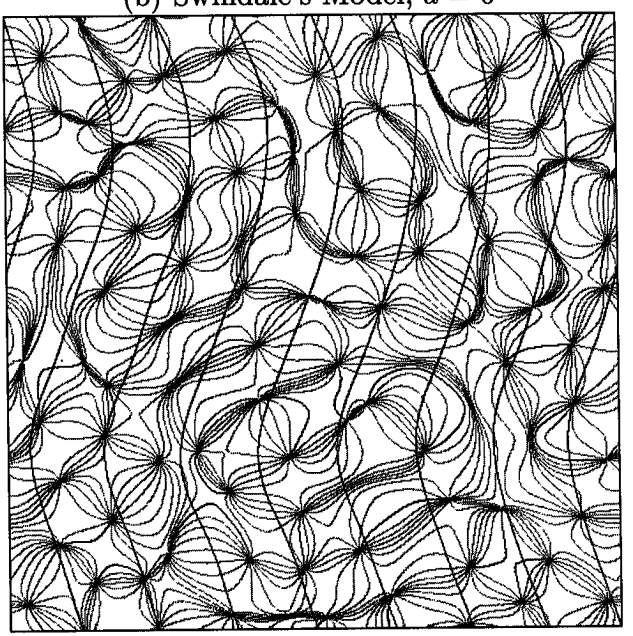

inputs in a random order causes a random choice among the possible stationary states and thus leads to global disorder.

3.4 Singularities and Linear Zones. Two features are prominent when visually inspecting the orientation map in Figure 1: singularities, points where all colors meet, and linear zones, regions with a rainbow appearance.

Singularities are point-like discontinuities in the orientation map, around which orientation preferences change by multiples of 180° along a closed loop. Macaque striate cortex contains only two types of singularities with vorticities[4] $+1/2$ and $-1/2$, respectively, with similar densities. All developmental models investigated so far generate maps that have this property. This is, however, not true for all of the structural models. Braitenberg's original proposal (Braitenberg 1985; Braitenberg and Braitenberg 1979), for example, included $+1$ singularities balanced by twice their density of $-1/2$ singularities, and the original icecube model (Hubel and Wiesel 1977) did not contain these features at all.

Linear zones are regions in the orientation map where isoorientation lines are (1) straight and run in parallel for a considerable distance, and where (2) isoorientation lines for similar intervals have similar spacing. With the help of a heuristic measure of "parallelness" that can be obtained by analyzing the gradients of orientation preference within small circular regions (see Obermayer 1993) it has been shown that linear zones are abundant in experimental maps. The existence of linear zones is related to the power spectrum. Linear zones are abundant only if the power spectrum has a strong bandpass characteristic, because linear zones are characterized by a periodic change of orientation preferences with distance. The ON/OFF competition model (Miller 1992, 1994) and the model of Tanaka (Miyashita and Tanaka 1992) generate maps with a power spectrum with significant energy in low-frequency modes, and lacking a significant bandpass characteristic. Linear zones thus appear less common

Figure 6: *Facing page.* (a) Model output from Swindale's (1992) spectral model in the same format as Figure 4. Model parameters (see Appendix): model size 512×512, $h_z = 1.32 \times 10^{-4} \exp[-(1.3r_1^2 + r_2^2)/1400] - 0.77 \times 10^{-4} \exp[-(r_1^2 + r_2^2)/2863]$, $h_\phi = 1.75 \times 10^{-4} \exp[-(r_1^2 + r_2^2)/823.0] - 1.06 \times 10^{-4} \exp[-(r_1^2 + r_2^2)/1646]$, $a = 20$. Initial values are normally distributed around 0 with variance 0.0025, map shown for $t = 500$ with $\alpha = 1.0$. The arrow indicates an area where an orientation column is distorted, or "kinked" at an ocular dominance band border. (b) Output from the same model with $a = 0$ (orientation and ocular dominance patterns not correlated); other parameters as in (a).

[4]Vorticity is defined as the factor of 360° by which orientation preferences increase (decrease) with counterclockwise movement around the center of positive (negative) vortices.

in these models than in macaque maps. Linear zones occur in all other models we studied, but are perhaps more prominent in the competitive Hebbian models than in macaque maps.

3.5 Anisotropies. Experimental patterns of orientation preference and ocular dominance are sometimes anisotropic, with elliptical, rather than circular, power spectra. In some species, such as macaque, the anisotropy in the ocular dominance pattern is strong enough to produce roughly parallel bands of ocular dominance across half of area 17 (Florence and Kaas 1992). In the cat the orientation preference patterns are anisotropic, while the ocular dominance bands are spotty and much less aligned (Andersen *et al.* 1988; Diao *et al.* 1990).

In models of cortical map formation anisotropies can emerge as a result of spontaneous symmetry breaking, pattern-generating equations that are not invariant under rotation, or through appropriately chosen boundary conditions. Models based on bandpass-filtered noise, for example, employ anisotropic kernels or filters (Niebur and Wörgötter 1993; Rojer and Schwartz 1990; Swindale 1980, 1992) (Fig. 6a,b). Feature maps (Durbin and Mitchison 1990; Goodhill and Willshaw 1990; Obermayer *et al.* 1990, 1992c) and some other models (Miller 1990; Miller *et al.* 1989) use anisotropic neighborhood or cortical-interaction functions (Fig. 7a). When the pattern-generating equations of a model are rotation invariant, anisotropic maps can still be produced using appropriate boundary conditions (Goodhill 1992) such as different shapes for the retina and cortex (Jones *et al.* 1991) (Fig. 7b) or perturbations of the model equations at the map edges, which can act as a seed leading to globally anisotropic maps (Swindale 1980; Tanaka 1991b). Interestingly, no models have yet been described that rely on spontaneous symmetry breaking to generate anisotropy.

3.6 Biases in Feature Preferences. The diversity principle, as stated above, must be modified to reflect that certain combinations of feature preferences are more common. For example, some experimenters have claimed that in certain or all layers of cortex more cells are responsive to a few particular orientations than to others (e.g., Bauer and Dow 1989). Other studies, including the optical imaging data from the superficial layers of V1 (Fig. 8) do not show any overrepresentation of a particular preferred orientation in the recorded areas (Finlay *et al.* 1976; Hubel and Wiesel 1968; Poggio *et al.* 1977). The optical imaging does, however, reveal a bias toward cells with high orientation specificity (Obermayer 1993).

While the experimental data are incomplete, it seems clear that all features are not represented equally. We find it instructive to consider how such biases can and have been introduced into existing models.

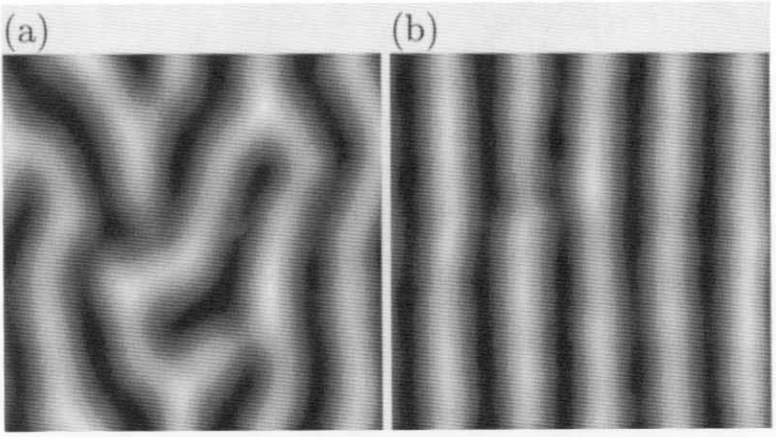

Figure 7: Anisotropic ocular dominance maps generated by the SOM-l algorithm. In (a) an anisotropic neighborhood function was used: $h_{\mathrm{SOM}}(\mathbf{r}, \mathbf{r}') = \exp\{-(r_1 - r_1')^2/(2\sigma^2) - (r_2 - r_2')^2/[2(1.3\sigma)^2]\}$, $\sigma = 16.97$. In (b) the effect of differing cortical and retinal shapes is simulated using a cortical sheet of size 512×512 and a retinal sheet of size 128×512. The initial values of $x(\mathbf{r})$ are amended to $x(\mathbf{r}) = 0.25 r_1$ and training patterns are drawn from $0 \leq v_x < 128$, $0 \leq v_y < 512$, $q_{\max} = 12.8$, $z_{\max} = 14.08$. Other parameters in (a) and (b) as in Figure 10.

Several structural models build in biases in preferred orientations (Bauer and Dow 1991; Braitenberg 1985; Dow and Bauer 1984). Most other models could also be modified to favor certain features. In models where training patterns are used, sensory deprivation has been simulated by biases in the training set. Training biases lead to biases in feature preferences (Obermayer *et al.* 1992a), which may be consistent with experimental findings (Blakemore and van Sluyters 1975; Stryker *et al.* 1978).

Increased ability to control the distribution of specificities and feature preferences distinguishes iterative spectral models (Swindale 1982, 1992) from similar one-step models (Niebur and Wörgötter 1993; Rojer and Schwartz 1990). (See Appendix 5.2.1 and 5.2.2.) One-step models generate a single, fixed distribution of orientation specificities (taken as orientation vector length) (Fig. 9a). Although optical imaging tends to underestimate orientation specificities through spatial averaging, it still reveals a distribution favoring higher orientation specificity than the one-step spectral models predict (Fig. 9b).

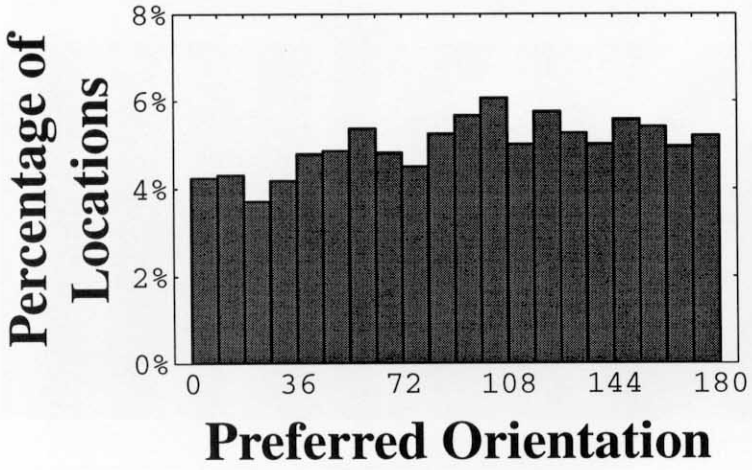

Figure 8: Histogram showing that preferred orientations in optical imaging data (animal NM1) are approximately evenly distributed. Each of 20 bins represents orientations in a 9° range.

Iterative spectral models allow the inclusion of functions linking development of distinct feature vector components and allow the possibility to reproduce any observed distribution of orientation specificities, preferred orientations, or ocularities, although so far no attempt has been made to precisely match experimental data. Linking functions can also be used to give correlations between otherwise independent feature components. Ultimately, however, the physiological basis of any linking function must be found if the model is to be used to predict map development.

3.7 Maps of Different Features Are Correlated. As explained in Section 2, the patterns of ocular dominance and orientation preference in macaque striate cortex are not independent. The two patterns are "globally orthogonal" such that the principal axes of the map patterns, measured on a length of about several ocular dominance bands, are not coincident, and may even be perpendicular. The two patterns also exhibit "local orthogonality" such that singularities and saddle points tend to align with the centers of ocular dominance bands, and isoorientation lines intersect ocular dominance band borders at approximately right angles.

Spectral models (Niebur and Wörgötter 1993; Rojer and Schwartz 1990; Swindale 1982, 1992) can be easily extended to include both ocular dominance and orientation preferences in three-dimensional feature

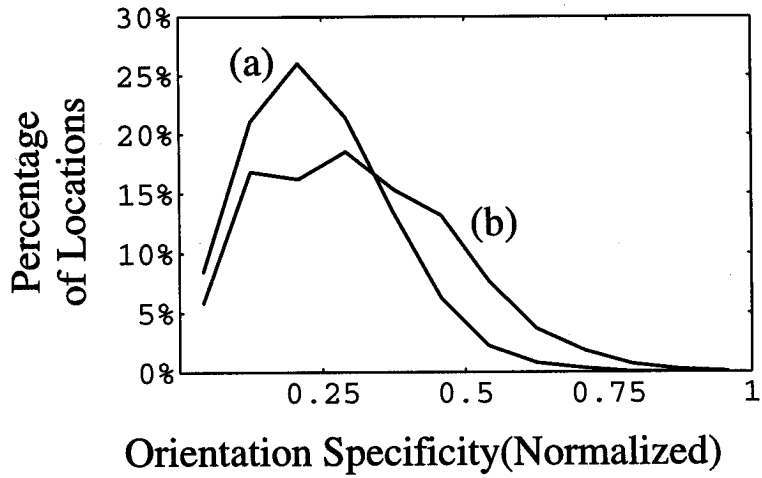

Figure 9: Histograms comparing the distribution of normalized orientation specificities q in maps from a one-step spectral model to experimental data. (a) One-step spectral models always generate a fixed distribution favoring low orientation specificities [data from the model of Niebur and Wörgötter (1993)]. (b) Optical imaging tends to underestimate orientation specificity compared to other experimental methods, yet still reveals a distribution favoring higher specificities than the one-step spectral models.

vectors. An array of these three-dimensional vectors can be componentwise convolved with a Mexican-hat kernel to generate ocular dominance and orientation preference patterns simultaneously. The two map patterns would not, however, be correlated unless the feature components were linked during pattern generation.

The Appendix (5.2.2) demonstrates two examples of linking functions that can be added to iterative spectral models. In a simple case, model cells are encouraged to develop (three-dimensional) feature vectors with approximately the same length. Thus cells with high monocularity will tend to have low orientation specificity and vice versa, which leads to the emergence of singularities in the centers of ocular dominance bands and to slabs of similar orientation preference intersecting ocular dominance borders preferentially at steep angles, i.e., local orthogonality.

A more physiologically interpretable linking function used by Swindale (1992) couples the separate feature components by reducing the speed at which orientation preference grows in regions where ocularity is high. Singularities with low orientation specificity will more likely

develop in the centers of single-eye dominance bands where growth of orientation preference was slowed (Fig. 6a). Figure 6a and b compares maps with and without the linking function. With the linking function, the otherwise distinct feature maps are locally coupled such that a tendency toward local orthogonality between isoorientation and ocular dominance borders develops.

Close inspection reveals several instances where the orientation preference map is distorted such that orientation domain borders are "kinked" at the ocular dominance band borders (Fig. 6a, see arrow). Such kinks are not seen in present macaque maps. Kinks in the model result from the specific linking function used. This linking function also predicts a course of development in which strong orientation preference occurs first along the ocular dominance borders, and develops more slowly in the monocular regions. No other known model produces these kinks. Thus, observation of such a pattern in future experimental data from any species would support this model's developmental hypothesis.

A simple extension (see Appendix 5.2.1) to the model of Rojer and Schwartz (1990), whereby both ocular dominance and orientation preference are derived from a single filtered noise array, generates maps with complete local orthogonality. Yet global orthogonality cannot be achieved in this simple model. Using an anisotropic filter would result in anisotropic map patterns, but both patterns would necessarily be elongated along the same axis.

Since Swindale's (1992) model allows different filters for the orientation and ocular dominance components, the wavelengths and anisotropies of the two patterns may be separately specified to give global orthogonality while still maintaining the same degree of local orthogonality. Although local and global orthogonality appear to be distinct properties of macaque maps, no other model currently treats them independently.

In simulations of the simultaneous development of orientation and ocular dominance, competitive Hebbian models (Figs. 10 and 11) generate patterns that include all of the types of local correlations between these two patterns that have been observed in the macaque, but do not reproduce global orthogonality.[5] These correlations have been demonstrated for the self-organizing map (Obermayer *et al.* 1992b,c) and are also present when the elastic-net approach (Durbin and Mitchison 1990) is appropriately extended (see Appendix 5.4.2). The correlations trivially emerge when patterns with the undesired combinations, e.g., low orientation specificity combined with binocularity, are excluded from the training set. However, they also occur when the training set includes all possible combinations of feature preferences.

For the latter case, the emergence of correlations between features can best be explained in the dimension-reduction framework (Fig. 12). In this framework cortical maps are described as mappings between a high-

[5]Global orthogonality, however, can be heuristically introduced by allowing different neighborhood functions to act on different components of the feature vector.

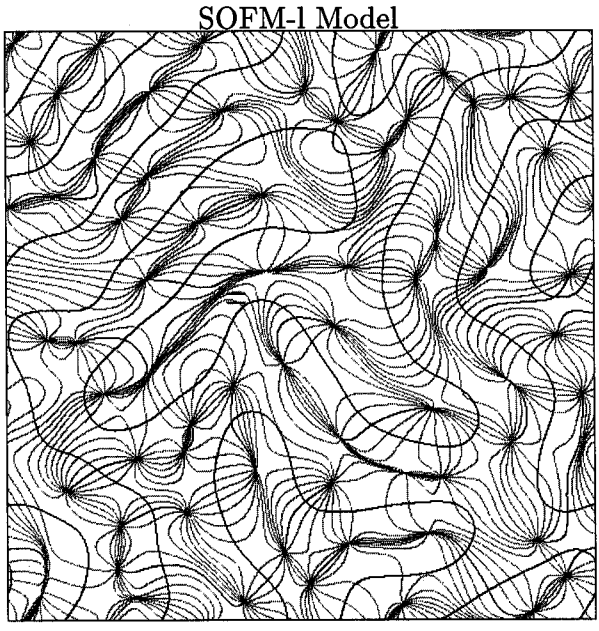

Figure 10: Model output from the self-organizing map (Obermayer *et al.* 1990, 1992c) in the format of Figure 4. Model size is 512 × 512 with periodic boundary conditions for the r_1 and r_2-axes. Training patterns $\mathbf{v} = \{v_x, v_y, v_q \sin(2v_\phi), v_q \cos(2v_\phi), v_z\}$ were chosen with uniform probability from $0 < v_x, v_y < 128$, $0 < v_\phi < \pi$, $0 < v_q < q_{\max}$, $|v_z| < z_{\max}$, $q_{\max} = 51.2$, $z_{\max} = 56.32$. Initial values: $x(\mathbf{r}) = r_1$, $y(\mathbf{r}) = r_2$, $q = 0.01 * q_{\max}$, $z = 0$, with ϕ uniformly distributed over all angles. In the function $h_{\mathrm{SOM}}(\cdot)$, $\sigma = 16.97$. Output is shown after 1,000,000 iterations with $\epsilon = 0.02$.

dimensional feature space and a two-dimensional cortical space that obey certain continuity and diversity constraints (Durbin and Mitchison 1990; Kohonen 1987; Obermayer *et al.* 1990). When training patterns are presented with equal probability out of an appropriate manifold in feature space, the magnification factor of the map between feature space and cortical coordinates will be approximately constant. Consequently, regions where one feature-vector component changes rapidly coincide with regions where other components change slowly. In regions where two feature components change fairly rapidly, they tend to do so along orthogonal axes in the cortex. If orientation selectivity and ocular dominance are represented by Cartesian coordinates as described in the Appendix,

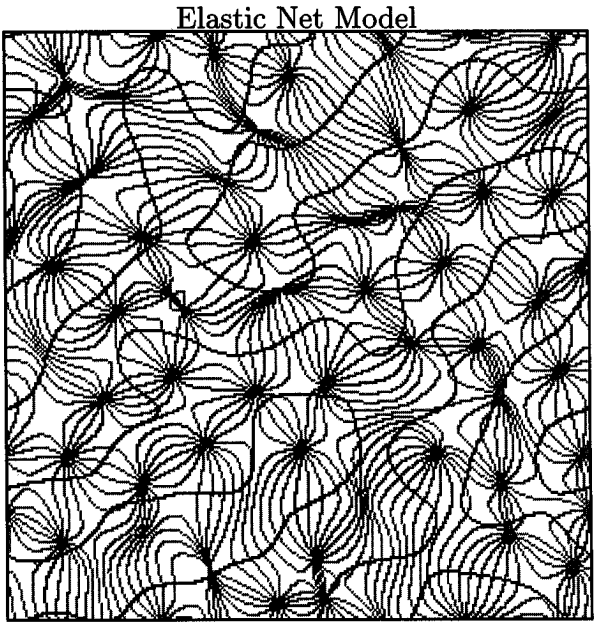

Figure 11: Model output from the elastic-net model (Durbin and Mitchison 1990) in the same format as Figure 4. Model size is 256×256 with periodic boundary conditions for r_1 and r_2. Initial values and training patterns as in Figure 10, with $q_{\max} = 61.44$, $z_{\max} = 46.08$. In the function $h_{\mathrm{EN}}(\cdot)$, $\sigma = 2.771$. Output is shown after 2,000,000 iterations with $\alpha = 0.4$, $\beta = 0.0001$.

the model maps will then develop with local orthogonality between orientation and ocular dominance columns, similar to what has been found in the macaque maps.

The generalized deformable model of Yuille (Yuille *et al.* 1991) can be made to produce similar maps to the elastic-net model. Yet he points out that the model may be generalized by modifying the definition of the norm used to enforce similarity between neighboring neurons. Different norms could lead to other types of correlations that might occur in other species, such as coincident regions of rapid change in orientation and ocular dominance.

The magnitude of the correlations between orientation preference and ocularity cannot be adequately determined from the current experimental data, because noise and slight movements of cortex during recording tend to destroy such correlations. Thus while we note that the SOM,

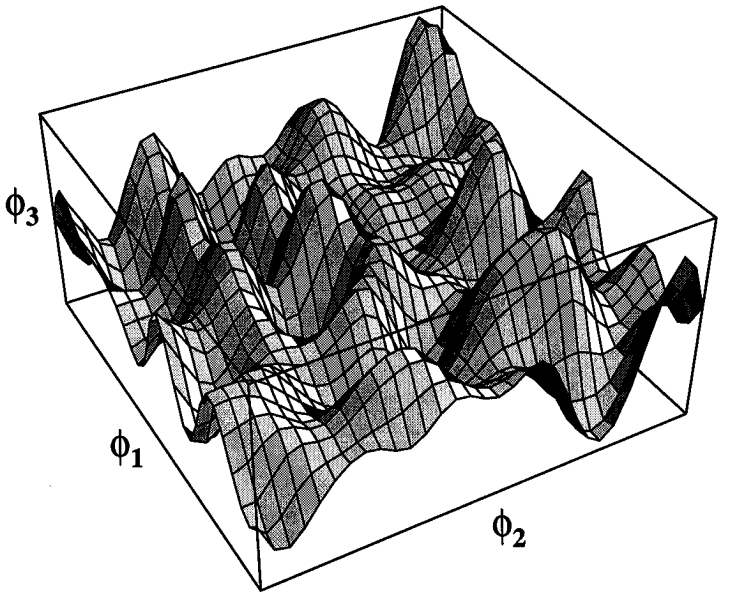

Figure 12: Dimension-reduction: This figure shows how points in a two-dimensional array might be mapped into a three-dimensional feature space with components ϕ_1, ϕ_2, and ϕ_3, representing such features as visual field location and ocular dominance. Dimension-reduction models often constrain the map to fill the input space with near-uniform density while maintaining continuity. This leads to maps where rapid changes in one feature vector component are correlated with slow changes in other vector components.

EN, and Rojer and Schwartz models predict stronger correlations than are observed experimentally, quantitative comparison is currently not recommended.

3.8 Correlations between Orientation Preference Coordinates and Cortical Coordinates. Several structural models imply particular relationships between the coordinate systems representing cortical location and orientation preference. For example, they may arrange cells preferring horizontal (or radial) stimuli in columns running in one direction across cortex while columns of cells preferring vertical (or concentric) stimuli run in the perpendicular direction (Bauer and Dow 1991; Dow and Bauer 1984).

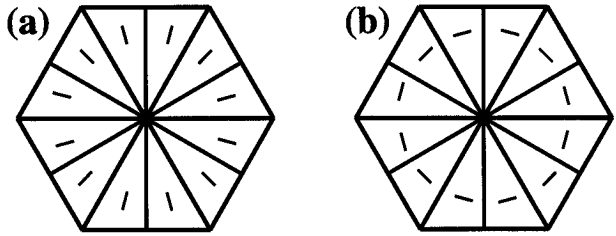

Figure 13: The pinwheel model (Braitenberg and Braitenberg 1979) tiles the plane with hexagonal hypercolumns each containing a +1 singularity. Six −1/2 singularities will be formed at the vertices where adjacent hypercolumns meet. Two versions of the model were suggested: (a) and (b). In each case, orientation preferences (short bars) are nearly perfectly correlated with the cortical orientation of the isoorientation lines (longer lines).

The implied link between coordinate systems is often visible if the maps are drawn using oriented line segments to directly represent preferred orientations of cells. Displaying maps from the pinwheel models (Braitenberg 1985; Braitenberg and Braitenberg 1979) in this way, line segments representing preferred orientations appear aligned along curves that either radiate out from, or circle around the +1 vortices (Fig. 13a and b). In this model, such an arrangement of the orientation selective cells arises from a simple, plausible scheme of synaptic connections. Although cortical maps are not as well ordered as this simplified model, this predicted link between cortical and retinal coordinates could be present to some degree.

A numerical test for such a link can be performed by comparing preferred orientations with the orientation of the isoorientation region contours. Alternatively the preferred orientations can be compared to the local orientation of the gradient vector of orientation preference with respect to cortical location, since this gradient vector is generally perpendicular to the isoorientation borders. In separate versions of the pinwheel model, the orientation preference vectors are either almost all perpendicular to (Fig. 13a) or almost all parallel to (Fig. 13b) the orientation gradient vectors. These trends are demonstrated in Figure 15g and h.

When analyzed in this way, the macaque optical imaging data show no preferred angle of intersection between orientation preference and its gradient vector (Fig. 15a) and thus no link between retinal and cortical coordinates.

Links between orientation preference and cortical coordinates are completely absent from models that treat orientation preference as an abstract

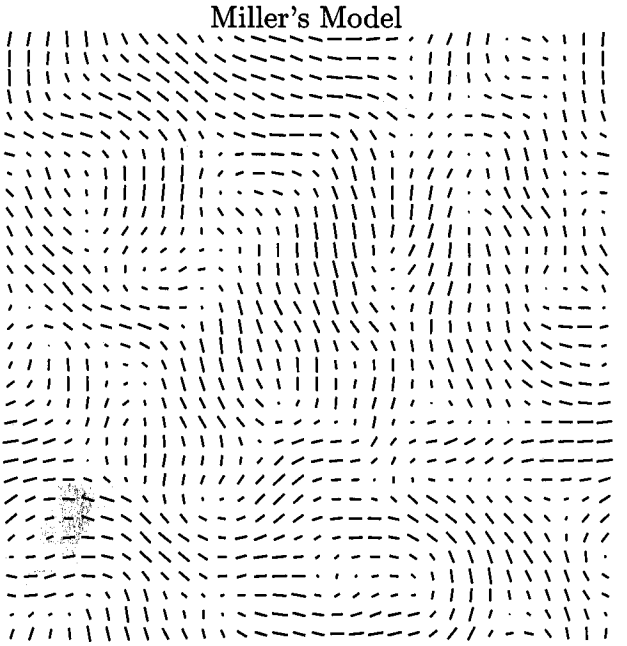

Figure 14: Orientation preference map from the correlation-based learning model of Miller (1992). Oriented lines represent the orientation preferences of an array of 32×32 cortical cells. Model parameters: $k_I = 1/9$, $\sigma_I = 3.0$, $C^{\text{same}}(\mathbf{x}, \mathbf{x}') = \exp(-\|\mathbf{x} - \mathbf{x}'\|/1.21) - (1/9)\exp(-\|\mathbf{x} - \mathbf{x}'\|/10.89)$, $C^{\text{diff}}(\mathbf{x}, \mathbf{x}') = (-1/2)C^{\text{same}}(\mathbf{x}, \mathbf{x}')$, arbor function $A(\mathbf{r}, \mathbf{x}) = \exp(-\|\mathbf{r} - \mathbf{x}\|/9.0)$. Initial synaptic weights were randomly distributed with uniform probability in the interval $1.6 < \Phi^i_{t=0}(\mathbf{r}, \mathbf{x}) < 2.4$. Map shown for $t = 900$ with $\alpha = 0.001$.

component of a feature vector, as in the spectral models (Fig. 15f) and the low-dimensional competitive Hebbian models (Fig. 15b). In models using the high-dimensional weight vector representation of receptive fields, a link often, but not necessarily, appears.

In one high-dimensional model (Miller 1992, 1994), cortical cells develop receptive fields with ON and OFF subfields, based on hypothetical correlations in the firing patterns of ON- and OFF-center geniculate cells (see Appendix 5.3). Orientation preferences result from alignment of the ON- and OFF-subfields, while intracortical interactions cause the orientation preferences of neighboring cells to be organized into a map across the cortical surface (Fig. 14). Although intended primarily as a model of development of single-cell orientation preferences, the model can ac-

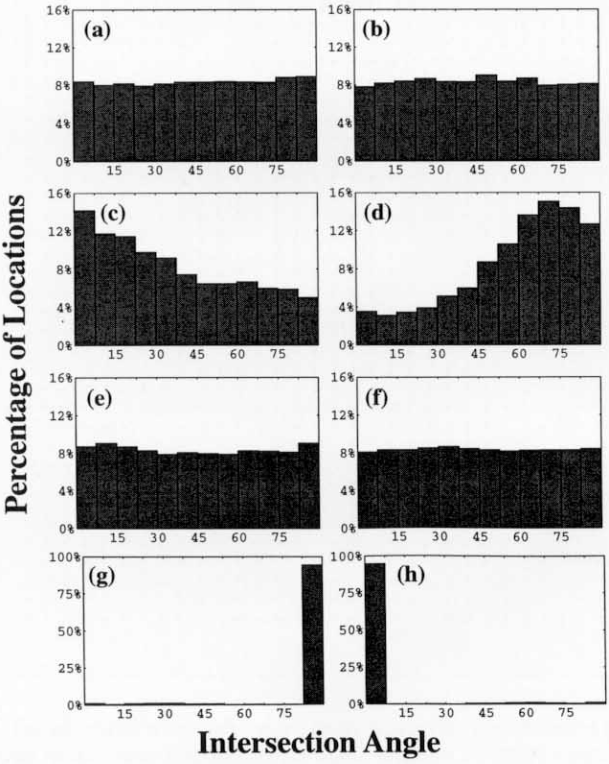

Figure 15: The histograms show the percentage of sites with a given difference angle $0 \leq I < 90°$ between preferred orientation $0 \leq \phi < 180°$ of a cortical cell and the orientation $0 \leq g < 180°$ on the cortical surface along which preferred orientation changes most rapidly. The difference angle is computed as $I = \min(|\phi - g|, 180° - |\phi - g|)$, where g is the angular component of the gradient $\mathbf{g} = [\nabla_{\mathbf{r}} \phi(\mathbf{r})] \bmod 180°$, approximated as $g_1 = 0.5[(\phi_{r_1+1,r_2} - \phi_{r_1-1,r_2}) \bmod 180°]$, $g_2 = 0.5[(\phi_{r_1,r_2+1} - \phi_{r_1,r_2-1}) \bmod 180°]$. (a) In experimental data (Fig. 4), and in competitive Hebbian models such as (b) the self-organizing map (Fig. 10), the difference angle takes on all values with equal probability. (c)–(d) Two correlation-based models predict a bias in the difference angles: (c) bias toward low I for Miller's model (Fig. 14) and (d) bias toward high I for Linsker's (1986c) model. (e) Tanaka's correlation-based model (Miyashita and Tanaka 1992) and (f) spectral models such as Swindale's model (Fig. 6a) predict an even distribution. (g) The two variants of the pinwheel model predict near 100% correlations with $I = 0$ for Figure 13a, and (h) $I = 90°$ for Figure 13b. Data for (d) described in Figure 2 of Linsker (1986c). These data contained only 10 distinct ϕ values, and had to be smoothed by gaussian filtering to allow computation of gradients. Data for (e) provided by S. Tanaka.

count for many of the prominent features of lateral map organization, like singularities, and fractures.

Analyzing the maps generated by this model as above reveals that there can occur a strong correlation between a cell's orientation preference in retinal coordinates and the orientation of the isoorientation bands in cortical coordinates. This results in orientation preference vectors aligned with the local direction of the orientation gradient (Fig. 15c) similar to but weaker than the correlations seen for the pinwheel model (Fig. 13b). Although the relationship has not been well studied, the strength of the correlations does depend on model parameters, and there appear to be some parameter regimes where such correlations are not apparent.

A related model by Linsker (1986c) produces maps that show a similar type of correlations (Fig. 15d) although in this case resembling the alternate version of the pinwheel model (Fig. 13a). As Linsker (1986c) noted, when cortical cells have receptive fields containing parallel subfields of opposing types, such as excitatory and inhibitory (likewise for ON and OFF), the degree of similarity between receptive fields will depend not only on their orientation but also on their relative location and internal structure. Two cortical cells with identical receptive field structure that are in partially overlapping locations in the retina would have greater similarity if they were displaced along the axis of the subfield alignment than if they were displaced along the perpendicular axis. Thus if the growth of receptive fields is influenced by the degree of receptive field similarity, correlations can develop between orientation preference (receptive field alignment) and the direction of orientation column alignment in cortex.

Tanaka's model of correlation-based learning (Tanaka 1991a; Miyashita and Tanaka 1992), as well as the high-dimensional version of the self-organizing map (Obermayer *et al.* 1990), are both similar to Miller's model in that orientation preferences develop through alignment of subregions in the receptive fields and growth of columnar structure is related to the overlap of receptive fields. We have examined data from one sample map from Tanaka's model and found that it did not show any correlations between retinal and cortical coordinates (Fig. 15e). We have likewise not observed the high-dimensional self-organizing map to predict a link between coordinate systems (Fig. 15b). It is unknown whether such a correlation could develop for some other choices of parameters.

Correlations between retinal and cortical coordinates are not seen in macaque maps (Fig. 15a) although they could be present in maps from other species. Since the measure of correlations introduced here has not previously been used to test model and experimental data, additional study will be required to determine the effect of model parameters on such correlations, and whether they occur in differently organized maps from other species.

Differences between the models above suggest a few tentative hypotheses. First, comparing the self-organizing map model and the mod-

els of Linsker and Miller suggests that the presence of contrasting types of subfields (ON/OFF or +/−) increases the likelihood that correlations will develop. The phase of two receptive fields will have less impact on their degree of overlap if there is a single type of subfield, as in the self-organizing map model. Second, the self-organizing map and Tanaka's models indicate that the inclusion of some scatter in the topographic projection from retinal to cortical locations could cause any correlation that may develop between the direction of subfield alignment and receptive field location in retinal coordinates to not be visible in the cortical map. Third, correlations appear to be more likely in models that consider only linear development rules, omitting refinements that could be due to more complex nonlinear processes.

3.9 Orientation Maps Are Not a Linear Transformation of a Conservative Vector Field. A spectral model proposed by Rojer and Schwartz (1990) used the gradient of a bandpass-filtered noise pattern to characterize cortical orientation maps (see Appendix 5.2.1). The model does generate maps that superficially resemble experimentally observed maps (Fig. 16). However, since the model maps are derived through a linear mapping from a conservative vector field (in which vectors are always perpendicular to the field gradient) the model predicts a unique type of link between cortical and orientation preference coordinates (Erwin *et al.* 1993). This relationship restricts the range of patterns the model can produce, as is easily demonstrated visually near singularities (Fig. 17).

One way to numerically demonstrate these correlations, and show that they are not present in macaque data, is to multiply the preferred orientations (180° periodic) in the maps by two to give a vector field (360° periodic). Analyzing the resulting vector field in a manner similar to the method of Figure 15 reveals that the direction of these vectors is strongly correlated with the direction of their gradient vector field for the model map. Similar correlations do not appear in spectral models that do not involve conservative vector fields (e.g., Niebur and Wörgötter 1993; Swindale 1982). However, such correlations do also occur in Götz's (1987) version of the pinwheel model. Analyzing the macaque data in a similar manner reveals that it cannot be derived from a linear mapping to a conservative field.

This discussion helps illuminate the utility of models that attempt to characterize map patterns in simple equations. Without Rojer and Schwartz's model it is unlikely that we would have noted that macaque orientation maps are not a linear function of a conservative vector field. Knowing this property of experimental maps, new models should be tested to ensure that such a relationship has not been unintentionally included.

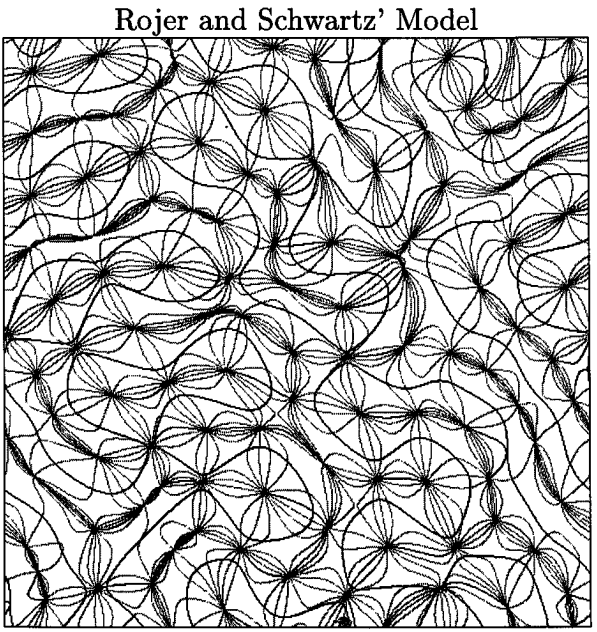

Figure 16: Orientation and ocular dominance map from a combined version of the models of Rojer and Schwartz (1990). Model size 512×512, $H(\mathbf{s}) = (1+e^{-\alpha*(\rho_c-\delta/2-\|\mathbf{s}\|)})^{-1} \times (1+e^{-\alpha*(\|\mathbf{s}\|-\rho_c-\delta/2)})^{-1}$, $\rho_c = 4.96$, $\delta = 0.96$, $\alpha = 1.5625$. Noise array $n(\mathbf{r})$ values are normally distributed around 0 with variance 1.0. Note that the medium gray orientation contour, which indicates 0°, exits all of the +1/2 singularities (exactly one-half of the singularities) from the left or right side only. See Figure 17 for an explanation.

4 Discussion

In this contribution we have investigated several models for the structure and the formation of orientation and ocular dominance maps. The results of our comparison between model predictions and experimental data obtained from the upper layers of macaque striate cortex are summarized in Table 2. References to articles on each model are given in Table 1. Many of the models are also briefly described in the Appendix.

Data for our comparisons come primarily from implementations of selected models on computers at our site. Generally our implementation followed closely the published description of the models and parameters. However, we extended a few models to include simultaneous

Table 2: Summary Comparison of Model Predictions[a]

	General Properties
Global disorder	Included in all models except several structural models (icecube, Götz, pinwheel)
Power spectrum	Miller, Yuille *et al.*, and Tanaka maps often have low-pass, rather than bandpass power spectra
Anisotropies	All models here can produce anisotropic map patterns
	Orientation Maps
Singularities	Absent from icecube model Arise spontaneously in many models of map formation Several structural models (Pinwheel, one form of Baxter and Dow) suggested 360° periodic singularities Overall orientations of singularities are restricted in Rojer and Schwartz
Saddle points	Absent only in icecube model
Fractures	Structural models tend to omit fractures All others include fractures as loci of rapid, continuous orientation change Miller, Linsker may include actual discontinuities, but the map resolution is too low to allow a meaningful distinction between rapid change and discontinuity
Linear zones/	Present to varying degrees in all models Less prominent in SOM-h, and correlation-based models
Linked coordinates	Pinwheel, Götz, and Baxter and Dow predict a link between a cell's preferred orientation and the direction of isoorientation columns For some parameters, Miller and Linsker suggest a similar link A link has not been observed in macaque data, nor in the remaining models
Conservative maps	Rojer and Schwartz, and Götz maps are a linear transformation of a conservative vector field Macaque maps, as well as other model maps, are not
Distribution of specificities	Most models that include a notion of feature specificity can be tuned to approximate experimentally observed distributions of specificity Among spectral models, the iterative approach (Swindale) allows finer control over the distribution of feature specificities than the one-step approach (Rojer and Schwartz, Niebur and Wörgötter)

[a]Model abbreviations are explained in Table 1.

Table 2: *Continued.*

Orientation deprivation and bias	Due to the method of learning by examples, competitive Hebbian models can easily simulate learning under exposure to a restricted or biased set of oriented visual features The other models here have not been applied to the same problem
Ocular Dominance	
Monocular deprivation	All models that include ocular dominance can simulate development or appearance of maps in monocularly deprived animals
Strabismus	Miller, SOM, EN, and Tanaka models successfully reproduce development of maps in strabismic animals
Relationships between Ocular Dominance and Orientation Maps	
Joint pattern development	Very few joint models of ocularity and orientation were proposed (SOM-h, SOM-l, Swindale) We have extended the EN and Rojer and Schwartz models to test their generalizability The model of Miller is currently being similarly extended, with no conclusive results at present
Orientation specificity and binocularity	All joint models correlate higher orientation specificity with binocularity and place singularities preferentially away from OD borders SOM-l, EN, and Rojer and Schwartz include a greater degree of correlation than observed in macaque
Local orthogonality	All joint models include some preference for ORI borders to be perpendicular to OD borders SOM-l, EN, and Rojer and Schwartz include a greater degree of correlation than observed in macaque Swindale's model makes a unique fine-scale prediction that has not been seen experimentally
Global orthogonality	Local and global orthogonality appear to be separate properties of experimental maps Only Swindale currently treats them separately in a model

development of orientation and ocular dominance so that we could compare them with the favorable results of the SOM models. We extended only several representative models where the extensions seemed to be a direct continuation of the model's principles and equations. Our extensions to the spectral model of Rojer and Schwartz, the correlation-based

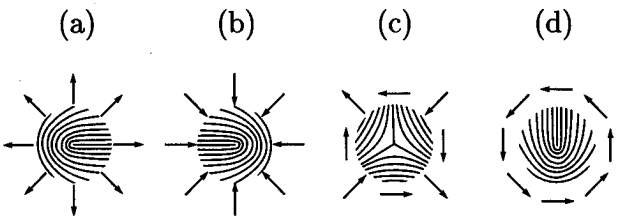

Figure 17: (a)–(d) Examples of vector fields (outside) and the associated orientation map (inside, local tangents to the curves) for typical singularities that can occur in the experimental data. The singularity (d) is an example of a feature not allowed by the model of Rojer and Schwartz (1990), because the curl of the associated vector field does not vanish at this location.

learning model of Miller, and the elastic-net model are described in Appendices 5.2.1, 5.3, and 5.4.2.

Among the pattern models, the spectral models perform better than the earlier structural models, mainly because they account for global disorder and for the coexistence of linear zones and singularities. The filtered noise approach for orientation selectivity (Niebur and Wörgötter 1993) and for ocular dominance (Rojer and Schwartz 1990) captures most of the important features of the individual maps, except for the high degree of feature selectivity that is observed in the macaque. Models by Swindale (1980, 1982, 1992) provide the currently best description of the individual orientation and ocular dominance patterns found in the macaque. Additionally, they can account for many correlations between the maps. Such a close match to experimental patterns has not yet been achieved in the more physiological high-dimensional models.

The particular form of the function used in Swindale's model to link development of orientation and ocular dominance leads to a prediction of occasional sudden changes in direction, or "kinks" in the isoorientation region borders at ocular dominance borders. This prediction is unique to Swindale's model. If such kinks are found in future high-resolution experimental images, it would support the model's prediction that orientation preference develops (or refines) first in binocular regions. Swindale's model is also unique in including separate mechanisms for generating local and global orthogonality. This extra freedom may be required to explain the structure of experimental maps.

Correlation-based learning models have led to valuable insight into the role of Hebbian learning in receptive field development (Linsker 1986a,b; Miller 1992; Yuille *et al.* 1989). They were not expected to predict the structure of cortical maps with as much precision. It is, however, in-

structive to note how the inclusion of realistic receptive field properties impacts on the cortical map patterns.

Correlation-based learning models perform well for ocular dominance (Miller *et al.* 1989). When applied to the formation of orientation maps (Linsker 1986c; Miller 1992), the ON/OFF-competition model underrepresents linear zones, and produces maps without a bandpass power spectrum. These points might be related to the low resolution of the maps necessitated by high computational demand.

Linsker's model always predicts a link between preferred orientation and direction of its vector gradient. Miller's model also predicts a link for some model parameters. Such a link is not present in the macaque data, thus constraining the range of parameters for which the model could apply to macaque data. If maps from different species are shown in the future to possess such a link, this would provide strong support for the correlation-based learning approach.

Competitive Hebbian models (Durbin and Mitchison 1990; Goodhill and Willshaw 1990; Obermayer *et al.* 1990, 1992c) lead to the currently best description of the observed patterns from a developmental perspective. These models attempt to describe the developmental process on a mesoscopic level, spatially as well as temporally, which has the advantage that the level of description matches the resolution of the experimental data. These models do not involve the microscopic concepts neuron, synapse, and spike, which makes it somewhat more difficult to relate model predictions to experimental data. Competitive Hebbian models make qualitatively correct predictions with respect to all the principles we have outlined above, except that they have not yet addressed the issue of global orthogonality as separate from local orthogonality. These models could be extended by, for example, including separate neighborhood functions for ocular dominance and orientation preference.

For correlations between orientation and ocular dominance maps, the competitive Hebbian models give the most realistic predictions. As expected, the predictions of the extended elastic-net model closely match the low-dimensional SOM algorithm. Since Yuille's generalized deformable model (Yuille *et al.* 1991) can be reduced to the elastic net, it should be equally capable of matching the experimental data if extended. Our extended version of the Rojer and Schwartz model failed to reproduce some of the experimentally observed correlations between orientation and ocularity. This observation is not intended to show a deficiency in their model as originally published. Rather, we wish to show how easily the property of local orthogonality and qualitatively correct correlations between singularities and ocularity emerge when the model is extended in a simple way. In our simulations with an extended version of the correlation-based learning model of Miller, maps with both well-organized orientation and ocular dominance failed to develop. We cannot, however, conclude that a more appropriate parameter regime does not exist. Further work on this joint model is in progress.

More stringent tests of the postulated mechanisms of activity-dependent neural development must rely on experiments that (1) monitor the actual timecourse of pattern formation and that (2) study pattern development under experimentally modified conditions (deprivation experiments). While progress has been made (Bonhoeffer *et al.* 1993; Löwel and Singer 1993; Hubel *et al.* 1977; Kim and Bonhoeffer 1993; Obermayer *et al.* 1994; Rauschecker 1991; Tanaka 1991b,c) there is currently not enough data on the spatial patterns available to constrain the present models. Unfortunately, no anatomical correlate has yet been found for orientation selectivity and binocularity in upper layers of monkey striate cortex. This quantity must be assessed physiologically and, therefore, after birth, which currently limits investigations to the final, refinement phase of orientation and ocular dominance development.

Further evidence to decide between proposed mechanisms might be derived from interspecies comparisons. The underlying assumption is that mechanisms of visual cortex development should be fairly universal and that any model of value should be able to account for interspecies variations. A few studies modeling cat and monkey patterns have been reported (Jones *et al.* 1991; Miller 1992; Obermayer *et al.* 1990; Rojer and Schwartz 1990; Swindale 1981). Yet, most studies focused on properties of the experimental patterns that arise from very basic assumptions like broken rotational symmetry, which leads to global map anisotropies. Consequently, most of the models were able to account for the observed interspecies variations. As more and better data become available (e.g., Blasdel *et al.* 1993), fewer of the existing models may continue to be useful.

Finally, one would like to have relatively simple models that make predictions about several aspects of cortical organization. Some current models do make predictions about features other than orientation preference and ocular dominance, such as receptive field location (Durbin and Mitchison 1990; Goodhill 1993; Jones *et al.* 1991; Obermayer *et al.* 1990, 1992c; Miyashita and Tanaka 1992; Yuille *et al.* 1991), color selectivity (Barrow and Bray 1992a), receptive field subfields, and spatial phase (Barrow and Bray 1992b; Berns *et al.* 1993; Linsker 1986c; Miller 1992, 1994; Miyashita and Tanaka 1992; Yuille *et al.* 1989), and correlations with locations of cytochrome-oxidase blobs (e.g., Götz 1988). Correlations between maps of different features are predicted by all of these models, and could be tested in suitably designed experiments.

5 Appendix: Model Descriptions

5.1 General Nomenclature. This Appendix gives brief formulations of several of the models included in this study. The model descriptions are intended to (1) ease comparison between different approaches by presenting models with common symbols, and (2) provide sufficient detail to allow interpretation of model parameters given in figure captions. By

necessity, the descriptions here reduce the complexity of some models. Refer to the original references for fuller descriptions and more general formulations.

Response properties of cortical cells or small cortical regions at each cortical location $\mathbf{r}$ are represented by a feature vector $\Phi(\mathbf{r})$. In the "low-dimensional" representation each component stands for a selected response property. Ocular dominance is represented by a scalar $z(\mathbf{r})$ where positive and negative numbers code for eye preferences and zero indicates binocularity. Preferred orientation $\phi(\mathbf{r})$ and degree of preference for that orientation $q(\mathbf{r})$ are denoted by more convenient Cartesian components $\phi(\mathbf{r}) = \{q(\mathbf{r})\sin[2\phi(\mathbf{r})], q(\mathbf{r})\cos[2\phi(\mathbf{r})]\}$ (Swindale 1982), where the factor of two enforces the assumption that the orientation maps code for the 180°-periodic orientation rather than the 360°-periodic direction of a stimulus.[6] Additional features, such as the retinal location $\{x(\mathbf{r}), y(\mathbf{r})\}$ of the receptive field or the preferred direction in color space, can be incorporated.

In the "high-dimensional" representation, the feature vector codes for the effective strength of the connections between a cortical cell and each of a set of N receptor cells in one or more input layers $\Phi(\mathbf{r}) = \{w_1(\mathbf{r}), w_2(\mathbf{r}), \ldots, w_N(\mathbf{r})\}$.

The subscript $\mathbf{r}$ for cortical location will be omitted in the equations below, except where necessary for clarity.

5.2 Spectral Models. Spectral models generate orientation and ocular dominance patterns by either convolving an array of random feature vectors with an appropriate kernel $h(\mathbf{r})$ in the space domain, or by filtering a noise array with an appropriate filter $H(\mathbf{s})$ in the Fourier domain. Convolution or filtering may be carried out either iteratively or in one step.

5.2.1 One-Step Spectral Models. The models of Rojer and Schwartz (1990). Let $n(\mathbf{r})$ be a white-noise pattern of independently chosen random numbers gaussian-distributed around 0 and let $h(\mathbf{r})$ be the space-domain representation of a bandpass filter $H(\mathbf{s})$. Then an ocular dominance-like pattern may be derived from

$$z = n.*h \tag{5.1}$$

where $*$ denotes convolution.

An orientation map is derived through a similar process by taking the vector gradient with respect to the cortical coordinates r_1 and r_2 of the filtered noise array. The preferred orientation ϕ is then taken as the angular direction of this vector divided by two, and in a simple extension

[6]This assumption is based in part on the appearance of the singularities.

of the model, an orientation specificity q may be taken from the length of the vector

$$\phi = (1/2)\tan^{-1}(u_2/u_1), q = \|\mathbf{u}\|, \qquad \text{where } \mathbf{u} = \left\{\frac{\partial z}{\partial r_1}, \frac{\partial z}{\partial r_2}\right\} \tag{5.2}$$

Due to the gradient operation, the orientation vector field is linearly related to a conservative field, and the model wrongly predicts correlations between orientation preferences and cortical locations such that

$$\oint q\sin(2\phi)dr_1 + q\cos(2\phi)dr_2 = 0 \tag{5.3}$$

is fulfilled for every closed path (Erwin *et al.* 1993). Rojer and Schwartz proposed separate models for orientation preference and ocular dominance, and omitted orientation specificity. For comparing their predictions with other models, we extend their model by considering $z(r)$ to be simultaneously an ocular dominance and the precursor of an orientation array, and consider q to represent orientation specificity.

The model of Niebur and Wörgötter (1993). An orientation map is derived by applying a bandpass filter $H(\mathbf{s})$ and an inverse Fourier transform *IFT* to a white-noise array $N(\mathbf{s})$ of independent, uniformly distributed elements in the Fourier domain. The Cartesian coordinates of the orientation vector are given by the real and imaginary parts of the resulting array Γ:

$$\Gamma = IFT(H \cdot N) \tag{5.4}$$

$$\{q\sin(2\phi), q\cos(2\phi)\} = \{Re(\Gamma), Im(\Gamma)\} \tag{5.5}$$

5.2.2 Iterative Spectral Models. Iterative models begin with a random distribution of small feature preferences $\|\Phi_0\| \ll 1$. A feature map develops through iterative application of an update equation

$$\Phi_{t+1} = \Phi_t + \alpha(\Phi_t * h)f(\Phi_t), \qquad 0 < \alpha < 1 \tag{5.6}$$

The function $f(\Phi)$ is chosen such that the components in Φ are appropriately coupled. A simple choice is

$$f(\Phi) = (1 - \|\Phi\|) \tag{5.7}$$

which encourages all feature vectors to grow toward a common length. If $\Phi = \{q\sin(2\phi), q\cos(2\phi), z\}$ then equations 5.6 and 5.7 lead to correlations between orientation selectivity and ocular dominance, which are qualitatively similar to the correlations observed in the macaque.

The models of Swindale. Swindale (1992) chose to exert finer control over the map structure by using differently sized Mexican-hat kernels h_z and h_ϕ for the ocular dominance and orientation components of Φ, and a more complicated coupling function f. His update equations read

$$z_{t+1} = z_t + \alpha(z_t * h_z)(1 - z_t^2) \tag{5.8}$$

$$\begin{aligned}\phi_{t+1} &= \{q\sin(2\phi), q\cos(2\phi)\} \\ &= \phi_t + \alpha(\phi_t * h_\phi)(1 - |z_t * h_z|)^a(1-q).\end{aligned} \tag{5.9}$$

For $a = 0$, equations 5.8 and 5.9 one recovers Swindale's independent models for ocular dominance (Swindale 1980) and orientation columns (Swindale 1982).

5.3 Correlation-Based Learning Models. We present several models by Miller to illustrate the principles of correlation-based learning. Miller's ocular dominance development model (Miller *et al.* 1989) uses a "high-dimensional" feature vector $\Phi^i(\mathbf{r}, \mathbf{x})$ coding for the strength of connection from each cortical location $\mathbf{r}$ to each retinal location $\mathbf{x}$ in each of two eyes $i \in \{0, 1\}$. Activity patterns in the retina are described by their two-point correlation function within, $C^{\text{same}}(\mathbf{x}, \mathbf{x}')$, and between, $C^{\text{diff}}(\mathbf{x}, \mathbf{x}')$, eyes, assuming that the coordinate systems in each eye are in one-to-one correspondence. The feature vectors are initialized, and then develop through an update equation, which in its simplest form is

$$\begin{aligned}\Phi^i_{t+1} &= \Phi^i_t + \alpha A(\mathbf{r}, \mathbf{x})[I * (C^{\text{same}} * \Phi^i_t) + I * (C^{\text{diff}} * \Phi^{1-i}_t)], \\ &\quad 0 < \alpha < 1\end{aligned} \tag{5.10}$$

The arbor function $A(\mathbf{r}, \mathbf{x})$ determines the location and overall size of the receptive fields. The intracortical interaction function $I(\mathbf{r}, \mathbf{r}')$ represents the effect of interactions between nearby cortical cells. It is often defined as

$$\begin{aligned}I(\mathbf{r}, \mathbf{r}') &= (0.5\delta(\|\mathbf{r} - \mathbf{r}'\|) + 0.5)[\exp(-\|\mathbf{r} - \mathbf{r}'\|^2/\sigma_I^2) \\ &\quad -k_I \exp(-\|\mathbf{r} - \mathbf{r}'\|^2/9\sigma_I^2)]\end{aligned} \tag{5.11}$$

where $\delta(\cdot)$ is the Kronecker delta function.

Generally, nonlinearities will be added to equation 10 through additional terms, normalization of weight vectors, or limiting the maximum and minimum values of each synaptic weight value.

Miller's model for orientation preference (Miller 1992, 1994) is formally similar, with the two feature vectors Φ^{ON} and Φ^{OFF} now representing connections to separate populations of ON- and OFF-center cells in the LGN. The two correlation functions C^{same} and C^{diff} again represent the expected correlations between cells at a given distance in the retina and of either the same or opposite cell types. The preferred orientations and orientation specificities are determined from the scalar product of the weight vectors with sinusoidal grating patterns.

For some parameters, e.g., for large σ_I, the model implies a link between coordinate systems that has not been seen in experimental data.

We have extended the model equations to include orientation and ocular dominance maps at the same time by including four separate types of synapses—two eyes with two types of ganglion cells in each. So far we have not found any set of correlation functions for which simulations lead to the coordinated growth of orientation and ocular dominance maps.

5.4 Competitive Hebbian Models. Competitive Hebbian models are based on essentially the same set of assumptions as correlation-based learning, with one crucial difference: the weighted summation of time-averaged cortical cell outputs via the lateral interaction function I, equations 10 and 5.11, is replaced by a nonlinear lateral interaction in which competition enhances the activity of units already highly activated in response to individual stimuli. The most prominent competitive Hebbian models are based on the self-organizing map (Kohonen 1982a,b) and the elastic net (Durbin and Willshaw 1987). Yuille's generalized deformable model can also be reduced to a competitive Hebbian model (Yuille *et al.* 1991) by appropriate choice of parameters.

5.4.1 Self-Organizing Map Models. The self-organizing map model (Obermayer *et al.* 1992c) employs an iterative procedure, in which low-dimensional feature vectors $\Phi = \{x, y, q\sin(2\phi), q\cos(2\phi), z\}$ are changed according to

$$\Phi_{t+1}(\mathbf{r}) = \Phi_t(\mathbf{r}) + \alpha h_{\mathrm{SOM}}(\mathbf{r}, \mathbf{r}')[\mathbf{v}_{t+1} - \Phi_t(\mathbf{r})], \qquad 0 < \alpha < 1 \tag{5.12}$$

At each iteration the stimulus $\mathbf{v}$ is chosen at random according to a given probability distribution $P(\mathbf{v})$. The function $h_{\mathrm{SOM}}(\cdot)$ is given by

$$\begin{aligned} h_{\mathrm{SOM}}(\mathbf{r}, \mathbf{r}') &= \exp(-\|\mathbf{r} - \mathbf{r}'\|^2/2\sigma^2), \\ \mathbf{r}'(\mathbf{v}, \{\Phi(\mathbf{r})\}) &= \min_{\mathbf{r}} d(\mathbf{v}, \Phi(\mathbf{r})) \end{aligned} \tag{5.13}$$

where $d(\cdot, \cdot)$ denotes the Euclidean distance.

A "high-dimensional" variant of the self-organizing map involves synaptic weights $\Phi(\mathbf{r}) = \{w_1(\mathbf{r}), w_2(\mathbf{r}), \ldots, w_N(\mathbf{r})\}$. In this model equation 5.12 is modified to

$$\Phi_{t+1}(\mathbf{r}) = \frac{\Phi_t(\mathbf{r}) + \alpha h_{\mathrm{SOM}}(\mathbf{r}, \mathbf{r}')\mathbf{v}_{t+1}}{\|\Phi_t(\mathbf{r}) + \alpha h_{\mathrm{SOM}}(\mathbf{r}, \mathbf{r}')\mathbf{v}_{t+1}\|}, \qquad 0 < \alpha < 1 \tag{5.14}$$

with the distance function in equation 5.13 replaced by $d(\mathbf{v}, \Phi) = 1 - \mathbf{v} \cdot \Phi$.

5.4.2 The Elastic-Net Model. The elastic-net algorithm (Durbin and Mitchison 1990; Durbin and Willshaw 1987) is an iterative procedure with the update rule:

$$\begin{aligned} \Phi_{t+1}(\mathbf{r}) &= \Phi_t(\mathbf{r}) + \alpha h_{\mathrm{EN}}(\mathbf{r}, \mathbf{v}_{t+1})[\mathbf{v}_{t+1} - \Phi_t(\mathbf{r})] \\ &\quad + \sum_{\|\mathbf{r}' - \mathbf{r}\| = 1} \beta[\Phi_t(\mathbf{r}') - \Phi_t(\mathbf{r})] \end{aligned} \tag{5.15}$$

with

$$h_{\mathrm{EN}}(\mathbf{r}, \mathbf{v}_{t+1}) = \exp\{-d[\mathbf{v}_{t+1}, \Phi(\mathbf{r})]^2/2\sigma^2\} / \sum_{\mathbf{r}'} h_{\mathrm{EN}}(\mathbf{r}, \mathbf{v}_{t+1}) \tag{5.16}$$

$d(\cdot,\cdot)$ is Euclidean distance. At each iteration, a stimulus $\mathbf{v}$ is chosen at random according to a given probability distribution $P(\mathbf{v})$.

We have extended previous modeling studies (Durbin and Mitchison 1990; Goodhill and Willshaw 1990) to include five-dimensional feature vectors $\Phi = \{x, y, q\sin(2\phi), q\cos(2\phi), z\}$. The extended model correctly predicts some of the correlations between the orientation and ocular dominance maps (Fig. 11).

Acknowledgments

This research has been supported by NSF (Grant 91-22522) and NIH (Grant P41RRO5969). Computer time on a CM-2 and a CM-5 was provided by the National Center for Supercomputing Applications, funded by NSF. Financial Support to E.E. by the Beckman Institute and to K.O. by ZiF (Universität Bielefeld) is gratefully acknowledged. We deeply appreciate model data supplied by R. Linsker, described in Linsker (1986c), and S. Tanaka (unpublished data). We thank K. Miller, E. Niebur, and A. Yuille for useful comments and discussions, and J. Malpeli for comments on the manuscript.

References

Adelson, E. H., and Bergen, J. R. 1985. Spatiotemporal energy models for the perception of motion. *J. Opt. Soc. Am. A* **2**, 284–299.

Andersen, P., Olavarria, J., and van Sluyters, R. C. 1988. The overall pattern of ocular dominance bands in cat visual cortex. *J. Neurosci.* **8**, 2183–2200.

Barrow, H. G., and Bray, A. J. 1992a. Activity-induced "colour blob" formation. In *Artificial Neural Networks II: Proceedings of the International Conference on Artificial Neural Networks*, I. Aleksander and J. Taylor, eds. Elsevier, Amsterdam.

Barrow, H. G., and Bray, A. J. 1992b. A model of adaptive development of complex cortical cells. In *Artificial Neural Networks II: Proceedings of the International Conference on Artificial Neural Networks*, I. Aleksander and J. Taylor, eds. Elsevier, Amsterdam.

Bartfeld, E., and Grinvald, A. 1992. Relationship between orientation-preference pinwheels, cytochrome oxidase blobs, and ocular dominance columns in primate striate cortex. *Proc. Natl. Acad. Sci. U.S.A.* **89**, 11905–11909.

Bauer, R., and Dow, B. M. 1989. Complementary global maps for orientation coding in upper and lower layers of the monkey's foveal striate cortex. *Exp. Brain Res.* **76**, 503–509.

Bauer, R., and Dow, B. M. 1991. Local and global principles of striate cortical organization: An advanced model. *Biol. Cybern.* **64**, 477–483.

Baxter, W. T., and Dow, B. M. 1989. Horizontal organization of orientation-sensitive cells in primate visual cortex. *Biol. Cybern.* **61**, 171–182.

Berns, G. S., Dayan, P., and Sejnowski, T. J. 1993. A correlational model for the development of disparity selectivity in visual cortex that depends on prenatal and postnatal phases. *Proc. Natl. Acad. Sci. U.S.A.* **90**, 8277–8281.

Blakemore, C., and van Sluyters, R. C. 1975. Innate and environmental factors in the development of the kitten's visual cortex. *J. Physiol. (London)* **248**, 663–716.

Blasdel, G. G. 1992a. Differential imaging of ocular dominance and orientation selectivity in monkey striate cortex. *J. Neurosci.* **12**(8), 3115–3138.

Blasdel, G. G. 1992b. Orientation selectivity, preference and continuity in monkey striate cortex. *J. Neurosci.* **12**(8), 3139–3161.

Blasdel, G. G., and Salama, G. 1986. Voltage sensitive dyes reveal a modular organization in monkey striate cortex. *Nature (London)* **321**, 579–585.

Blasdel, G. G., Livingstone, M., and Hubel, D. 1993. Optical imaging of orientation and binocularity in visual areas 1 and 2 of squirrel monkey (Samiri sciureus) cortex. *Soc. Neurosci. Abstr.* **19**, 1500.

Blasdel, G. G., Obermayer, K., and Kiorpes, L. 1994. Organization of ocular dominance and orientation columns in the striate cortex of neonatal macaque monkeys. *Vis. Neurosci.*, in press.

Bonhoeffer, T., Kim, D., and Singer, W. 1993. Optical imaging of the reverse suture effect in kitten visual cortex during the critical period. *Soc. Neurosci. Abstr.* **19**, 1800.

Braitenberg, V. 1985. An isotropic network which implicitly defines orientation columns: Discussion of an hypothesis. In *Models of the Visual Cortex*, D. Rose and V. G. Dobson, eds., pp. 479–484. John Wiley, New York.

Braitenberg, V., and Braitenberg, C. 1979. Geometry of orientation columns in the visual cortex. *Biol. Cybern.* **33**, 179–186.

Diao, Y.-C., Jia, W. G., Swindale, N. V., and Cynader, M. S. 1990. Functional organization of the cortical 17/18 border region in the cat. *Exp. Brain Res.* **79**, 271–282.

Dow, B. W., and Bauer, R. 1984. Retinotopy and orientation columns in the monkey: A new model. *Biol. Cybern.* **49**, 189–200.

Durbin, R., and Mitchison, G. 1990. A dimension reduction framework for understanding cortical maps. *Nature (London)* **343**, 341–344.

Durbin, R., and Willshaw, D. 1987. An analogue approach to the traveling salesman problem using an elastic net method. *Nature (London)* **326**, 689–691.

Emerson, R. C., Bergen, J. R., and Adelson, E. H. 1992. Directionally selective complex cells and the computation of motion energy in cat visual cortex. *Vision Res.* **32**(2), 203–218.

Erwin, E., Obermayer, K., and Schulten, K. 1993. A comparison of models of visual cortical map formation. In *Computation and Neural Systems*, F. H. Eeckman and J. M. Bower, eds., ch. 60, pp. 395–402. Kluwer Academic Publishers, Dordrecht.

Finlay, B. L., Schiller, P. H., and Volman, S. F. 1976. Meridional differences in orientation sensitivity in monkey striate cortex. *Brain Res.* **105**, 350–352.

Florence, S. L., and Kaas, J. H. 1992. Ocular dominance columns in area 17 of

Old World macaque and talapoin monkeys: Complete reconstructions and quantitative analyses. *Vis. Neurosci.* **8**, 449–462.

Goodhill, G. J. 1992. Correlations, competition, and optimality: Modelling the development of topography and ocular dominance. Ph.D. thesis, University of Sussex at Brighton.

Goodhill, G. J. 1993. Topography and ocular dominance: A model exploring positive correlations. *Biol. Cybern.* **69**, 109–118.

Goodhill, G. J., and Willshaw, D. J. 1990. Application of the elastic net algorithm to the formation of ocular dominance stripes. *Network* **1**, 41–59.

Goodman, C., and Shatz, C. 1993. Developmental mechanisms that generate precise patterns of neuronal connectivity. *Cell* **72**, 77–89.

Götz, K. G. 1987. Do "d-blob" and "l-blob" hypercolumns tessellate the monkey visual cortex? *Biol. Cybern.* **56**, 107–109.

Götz, K. G. 1988. Cortical templates for the self-organization of orientation-specific d- and l-hypercolumns in monkeys and cats. *Biol. Cybern.* **58**, 213–223.

Grinvald, A., Lieke, E., Frostig, R. P., Gilbert, C., and Wiesel, T. 1986. Functional architecture of cortex revealed by optical imaging of intrinsic signals. *Nature (London)* **324**, 351–354.

Hubel, D., and Wiesel, T. N. 1962. Receptive fields, binocular interaction and functional architecture in the cat's striate cortex. *J. Physiol. (London)* **160**, 106–154.

Hubel, D. H., and Wiesel, T. N. 1968. Receptive fields and functional architecture of monkey striate cortex. *J. Physiol.* **195**, 215–243.

Hubel, D., and Wiesel, T. N. 1974. Sequence regularity and geometry of orientation columns in monkey striate cortex. *J. Comp. Neurol.* **158**, 267–293.

Hubel, D., and Wiesel, T. N. 1977. Functional architecture of monkey striate cortex. *Proc. Roy. Soc. London B* **198**, 1–59.

Hubel, D., Wiesel, T. N., and LeVay, S. 1977. Plasticity of ocular dominance columns in monkey striate cortex. *Phil. Trans. Roy. Soc. Lond. B* **278**, 377–409.

Hubel, D., Wiesel, T. N., and Stryker, M. 1978. Anatomical demonstration of orientation columns in macaque monkey. *J. Comp. Neurol.* **177**, 361–380.

Jones, D. G., van Sluyters, R. C., and Murphy, K. M. 1991. A computational model for the overall pattern of ocular dominance. *J. Neurosci.* **11**(12), 3794–3808.

Kim, D., and Bonhoeffer, T. 1993. Chronical observation of the emergence of iso-orientation domains in kitten visual cortex. *Soc. Neurosci. Abstr.* **19**, 1800.

Kohonen, T. 1982a. Analysis of a simple self-organizing process. *Biol. Cybern.* **44**, 135–140.

Kohonen, T. 1982b. Self-organized formation of topologically correct feature maps. *Biol. Cybern.* **43**, 59–69.

Kohonen, T. 1987. *Self-Organization and Associative Memory.* Springer-Verlag, New York.

Lehky, S. R., Sejnowski, T. J., and Desimone, R. 1992. Predicting responses of nonlinear neurons in monkey striate cortex to complex patterns. *J. Neurosci.* **12**(9), 3568–3581.

LeVay, S., and Nelson, S. B. 1991. The columnar organization of visual cortex.

In *The Electrophysiology of Vision*, A. Leventhal, ed., pp. 15–34. Macmillan, London.

Linsker, R. 1986a. From basic network principles to neural architecture: Emergence of spatial opponent cells. *Proc. Natl. Acad. Sci. U.S.A.* **83**, 7508–7512.

Linsker, R. 1986b. From basic network principles to neural architecture: Emergence of orientation selective cells. *Proc. Natl. Acad. Sci. U.S.A.* **83**, 8390–8394.

Linsker, R. 1986c. From basic network principles to neural architecture: Emergence of orientation columns. *Proc. Natl. Acad. Sci. U.S.A.* **83**, 8779–8783.

Livingstone, M., and Hubel, D. 1984. Anatomy and physiology of a color system in the primate visual cortex. *J. Neurosci.* **4**, 309–356.

Löwel, S., and Singer, W. 1993. Strabismus changes the spacing of ocular dominance columns in the visual cortex of cats. *Soc. Neurosci. Abstr.* **19**, 359.2.

Miller, K. D. 1990. Correlation based models of neural development. In *Neuroscience and Connectionst Theory*, M. Gluck and D. Rumelhart, eds., pp. 267–354. Lawrence Erlbaum, Hillsdale, NJ.

Miller, K. D. 1992. Development of orientation columns via competition between on- and off-center inputs. *NeuroReport* **3**, 73–76.

Miller, K. D. 1994. A model for the development of simple cell receptive fields and the ordered arrangement of orientation columns through activity-dependent competition between on- and off-center inputs. *J. Neurosci.* **14**, 409–441.

Miller, K. D., Keller, J. B., and Stryker, M. P. 1989. Ocular dominance column development: Analysis and simulation. *Science* **245**, 605–615.

Miyashita, M., and Tanaka, S. 1992. A mathematical model for the self-organization of orientation columns in visual cortex. *NeuroReport* **3**(1), 69–72.

Niebur, E., and Wörgötter, F. 1993. Orientation columns from first principles. In *Computation and Neural Systems*, F. H. Eeckman and J. M. Bower, eds., ch. 62, pp. 409–413. Kluwer Academic Publishers, Dordrecht.

Obermayer, K. 1993. *Adaptive Neuronale Netze und ihre Anwendung als Modelle der Entwicklung Kortikaler Karten*. Infix–Verlag, St. Augustin.

Obermayer, K., and Blasdel, G. G. 1993. Geometry of orientation and ocular dominance columns in monkey striate cortex. *J. Neurosci.* **13**, 4114–4129.

Obermayer, K., Ritter, H., and Schulten, K. 1990. A principle for the formation of the spatial structure of cortical feature maps. *Proc. Natl. Acad. Sci. U.S.A.* **87**, 8345–8349.

Obermayer, K., Ritter, H., and Schulten, K. 1992a. A model for the development of the spatial structure of retinotopic maps and orientation columns. *IEICE Trans. Fund. Electr. Comm. Comp. Sci.* **E75-A**(5), 537–545.

Obermayer, K., Schulten, K., and Blasdel, G. G. 1992b. A comparison between a neural network model for the formation of brain maps and experimental data. In *Advances in Neural Information Processing Systems 4*, D. S. Touretzky and R. Lippman, eds., pp. 83–90. Morgan Kaufmann, San Mateo, CA.

Obermayer, K., Blasdel, G. G., and Schulten, K. 1992c. Statistical mechanical analysis of self-organization and pattern formation during the development of visual maps. *Phys. Rev. A* **45**(10), 7568–7589.

Obermayer, K., Kiorpes, L., and Blasdel, G. G. 1994. Development of orientation and ocular dominance columns in infant macaques. In *Advances in Neural Information Processing Systems 6*, J. D. Cowan, G. Tesauro, and J. Alspector, eds., pp. 543–550. Morgan Kaufmann, San Mateo, CA.

Poggio, G. F., Doty, R. W., Jr., and Talbot, W. H. 1977. Foveal striate cortex of behaving monkey single neuron responses to square wave gratings during fixation of gaze. *J. Neurophysiol.* **40**(6), 1369–1391.

Rauschecker, J. 1991. Mechanisms of visual plasticity: Hebb synapses, NMDA receptors, and beyond. *Physiol. Rev.* **71**, 587–615.

Reggia, J., D'Autrechy, C. L., Sutton, G., and Weinrich, M. 1992. A competitive distribution theory of neocortical dynamics. *Neural Comp.* **4**, 287–317.

Rojer, A. S., and Schwartz, E. L. 1990. Cat and monkey cortical columnar patterns modeled by bandpass-filtered 2d white noise. *Biol. Cybern.* **62**, 381–391.

Sirosh, J., and Miikkulainen, R. 1994. Cooperative self-organization of afferent and lateral connections in cortical maps. *Biol. Cybern.* **71**, 66–78.

Stryker, M. P., Sherk, H., Leventhal, A. G., and Hirsch, H. V. B. 1978. Physiological consequences for the cat's visual cortex of effectively restricting early visual experience with oriented contours. *J. Neurophysiol.* **41**, 896–909.

Swindale, N. V. 1980. A model for the formation of ocular dominance stripes. *Proc. Royal Soc. London B* **208**, 243–264.

Swindale, N. V. 1981. Rules for pattern formation in mammalian visual cortex. *Trends Neurosci.* **4**, 102–104.

Swindale, N. V. 1982. A model for the formation of orientation columns. *Proc. Royal Soc. London B* **215**, 211–230.

Swindale, N. V. 1991. Coverage and the design of striate cortex. *Biol. Cybern.* **65**, 415–424.

Swindale, N. V. 1992. A model for the coordinated development of columnar systems in primate striate cortex. *Biol. Cybern.* **66**, 217–230.

Swindale, N. V., Matsubara, J. A., and Cynader, M. S. 1987. Surface organization of orientation and direction selectivity in cat area 18. *J. Neurosci.* **7**, 1414–1427.

Tanaka, S. 1991a. Information among ocularity, retinotopy and on-/off-center pathways. In *Advances in Neural Information Processing Systems 3*, R. P. Lippman *et al.*, eds., pp. 18–25. Morgan Kaufmann, San Mateo, CA.

Tanaka, S. 1991b. Phase transition theory for abnormal ocular dominance column formation. *Biol. Cybern.* **65**, 91–98.

Tanaka, S. 1991c. Theory of ocular dominance column formation: Mathematical basis and computer simulation. *Biol. Cybern.* **64**, 263–272.

Tootell, R. B. H., *et al.* 1988. Functional-anatomy of macaque striate cortex. (series). *J. Neurosci.* **8**(5), 1500–1624.

Ts'o, D. Y., Frostig, R. D., Lieke, E. E., and Grinvald, A. 1990. Functional organization of primate visual cortex revealed by high resolution optical imaging. *Science* **249**, 417–420.

Yuille, A. L., Kammen, D. M., and Cohen, D. S. 1989. Quadrature and the de-

velopment of orientation selective cortical cells by Hebb rules. *Biol. Cybern.* **61**, 183–194.

Yuille, A. L., Kolodny, J. A., and Lee, C. W. 1991. *Dimension reduction, generalized deformable models and the development of ocularity and orientation.* Tech. Rep. 91-3, Harvard Robotics Laboratory.

Received February 7, 1994; accepted September 19, 1994.